CONSTELLATION PHARMACOLOGY OF TRPM8- AND TRPA1-EXPRESSING SOMATOSENSORY NEURONS

by

Tosifa Memon

A dissertation submitted to the faculty of
The University of Utah
in partial fulfillment of the requirements for the degree of

Doctor of Philosophy

Department of Biology

The University of Utah

August 2017

The University of Utah Graduate School

STATEMENT OF DISSERTATION APPROVAL

The dissertation of **Tosifa Memon**

has been approved by the following supervisory committee members:

Baldomero M Olivera	, Chair	**04/18/2017** Date Approved
Russell W Teichert	, Member	**04/18/2017** Date Approved
Franz Goller	, Member	**04/18/2017** Date Approved
David Krizaj	, Member	**04/18/2017** Date Approved
Christopher Reilly	, Member	**04/18/2017** Date Approved

and by **Denise Dearing** , Chair/Dean of

the Department/College/School of **Biology**

and by David B. Kieda, Dean of The Graduate School.

ABSTRACT

Constellation pharmacology is an imaging platform that can be used to identify functionally relevant cell-types based on cell-specific combinations (constellations) of key signaling proteins, and to screen for novel pharmacological agents that target these proteins and cell-types. In this dissertation, cold-sensitive somatosensory neurons expressing TRPM8 and TRPA1 channels were identified and studied from rodent dorsal root ganglia and trigeminal ganglia. We have identified constellations of ion channels functionally expressed in TRPM8- and TRPA1-expressing neurons, which has provided novel insight into the role of these neurons in cold-sensation. Our results are consistent with the model where TRPM8-expressing neurons contribute to innocuous cold-sensation and cold-sensitive TRPA1-expressing neurons contribute to noxious cold-sensation. Using constellation pharmacology, we also identified the cellular and molecular target of sweet and licorice fennel oil and its major active compound *trans*-anethole. To our surprise, both fennel oil and *trans*-anethole selectively target TRPA1-expressing neurons in mouse somatosensory neurons. Furthermore, both fennel oil and *trans*-anethole also activate human TRPA1 channels. Hence, this dissertation is a good case study for how constellation pharmacology can be used for cell-type identification and screening natural products for discovery.

I dedicate this dissertation to my doting parents, Shamim and Aziz, my caring sister, Tehsim (Rani), and my loving husband, Javed, along with other family members and friends for their love and support throughout this remarkable journey. Thank You!

TABLE OF CONTENTS

LIST OF TABLES

LIST OF FIGURES

ACKNOWLEDGEMENTS

I sincerely thank my advisor, Baldomero Olivera, for giving me the opportunity to work on this project and for continuous support throughout. I feel fortunate to have worked under Russell Teichert's mentorship. His encouragement and guidance kept me going even during rough times.

I am very grateful to Christopher Reilly for providing valuable input and resources, which proved instrumental in shaping this project. I am also thankful to past and present members of my supervisory committee, especially Franz Goller and David Krizaj for their critical and helpful comments throughout this project.

Working on this project has been a wonderful learning experience. This would not have been possible without my helpful and collaborative colleagues. I thank past and present members of the calcium imaging group, especially Kevin Chase for developing R program functions to expedite the data analysis. I am also thankful to Pradip Bandyopadhyay, Arik Hone, Shrinivasan (Cheenu) Raghuraman, Min-min Zhang, and Doju Yoshikami along with other members of the Olivera lab for their help at various stages of this project. Lastly, I would like to express my gratitude to Rocio Finol-Urdaneta for her brief but impactful training on single-cell RT-qPCR.

CHAPTER 1

INTRODUCTION

Is the sensation of cold temperature dependent on one molecular sensor that is expressed in a single neuronal cell type, or is it a more complex phenomenon that involves integration of information at multiple levels of the nervous system? In the past 20 years, a set of molecules from the Transient Receptor Potential (TRP) channel family have been discovered as sensors for cold, heat, pressure, etc. (Venkatachalam and Montell, 2007). How the information detected by these channels is integrated, leading to perception, has hardly been explored. To fill this gap, we studied cold-sensitive neurons and identified molecular players that influence cold-sensation.

Cold temperatures below 20°C primarily activate TRPM8 channels (Bautista et al., 2007; Dhaka et al., 2007). However, TRPM8-expressing neurons display a continuum of responses to cold stimuli (Madrid et al., 2009; Teichert et al., 2014). The variable threshold of TRPM8-expressing neurons to cold temperatures depends on the expression of TRPM8 and voltage-gated potassium (K_V) channels (Madrid et al., 2009; Teichert et al., 2014). High expression of TRPM8 and low expression of K_V channels results in low thresholds of cold sensitivity whereas low expression of TRPM8 channels and high expression of K_V channels results in high thresholds of cold-sensitivity. Hence, the coordination between TRPM8 and K_V channel expression, and their activity fine tunes the cold-sensitivity of TRPM8-expressing neurons.

Even though TRPM8 is activated by noxious cold temperature below 10°C, TRPM8-/- mice retain cold-sensitivity in this temperature range (Bautista et al., 2007; Colburn et al., 2007; Dhaka et al., 2007). Another TRP channel, TRPA1, has been implicated to detect these noxious cold temperatures (Story et al., 2003; Kwan et al., 2006; Fajardo et al., 2008; Karashima et al., 2009; Moparthi et al., 2014). However, the role of TRPA1 in

noxious cold-sensation has been debated for over a decade (McKemy, 2005; Caspani and Heppenstall, 2009; Vriens et al., 2014; Ran et al., 2016; Yarmolinsky et al., 2016). In Chapter 2, we investigate the role of TRPA1 in cold-sensation at the cellular level. We also determine the factors that contribute to cold-sensitivity of TRPA1-expressing neurons. Like TRPM8-expressing neurons, we find that the coordination of TRPA1 and K_V channel expression and their activity influence cold-sensitivity of TRPA1-expressing neurons.

Cold temperatures below 10°C can also affect voltage-gated sodium channels (Na_V). Most Na_V channel subtypes inactivate (become non-functional) under extreme cold except the $Na_V1.8$ channel, which makes it essential for excitability of neurons at temperatures below 10°C (Zimmermann et al., 2007). Hence, we studied the distribution of $Na_V1.8$ among TRPM8- and TRPA1-expressing neurons (Chapter 3). Besides cold, sodium channels also play an important role in pain sensation (Paper, 1999; Braz et al., 2005; Waxman, 2012; Dib-hajj et al., 2017). For instance, loss of $Na_V1.7$ function can lead to complete loss of pain sensation in humans and mice (Cox et al., 2006; Weiss et al., 2011; Gingras et al., 2014). Thus, we also developed novel calcium imaging-based experimental protocols and determined functional expression of TTX-S Na_V channels in TRPM8- and TRPA1-expressing neurons (Chapter 3).

As most TRP channels are targets of various tastants and odorants (Roper, 2014; Friedland and Harteneck, 2017), we screened activity of sweet and licorice Fennel oil in sensory neurons that express TRP channels. Despite wide use of fennel in cooking and baking, the molecular receptors responsible for its chemesthesis, taste, and flavor have not been identified (Badgujar et al., 2014). Using calcium imaging, we could identify the

cellular and molecular target of Fennel oil and its major component *trans*-anethole (Chapter 4). Both sweet Fennel oil and *trans*-anethole target TRPA1, a channel known to be targeted by pungent chemicals and environmental irritants (Jordt et al., 2004; Bautista et al., 2005; Deering-Rice et al., 2011). As fennel oil and *trans*-anethole produce a cooling sensation in the mouth, unlike other pungent TRPA1 agonists, such as mustard oil, this result was unexpected. I am in the process of exploring how two chemicals, *trans*-anethole (Sweet) and AITC (Pungent), that activate the same cell surface receptor (TRPA1 channels) result in different sensations. I provide some preliminary insights in Chapter 4.

Cumulatively, my dissertation research has demonstrated that the function of neuronal cell-types is not just dependent on a single ion channel but the specific combination (constellation) of ion channels. For instance, the identity of a cold-nociceptor does not only depend on the presence of a certain TRP channel but also depends on the modulation of TRP channel activity by K_V channels and downstream action potential firing by specific Na_V channel subtypes. Furthermore, identifying neuronal cell-types through constellation pharmacology expedited the discovery of the cellular and molecular targets of fennel oil and *trans*-anethole. In the future, we will continue to use the constellation pharmacology approach to investigate the differences in cell-specific constellations between normal versus diseased states, and to discover cellular and molecular targets of natural products.

1.1 References

Badgujar SB, Patel V V, Bandivdekar AH (2014) Foeniculum vulgare mill : a review of its botany, phytochemistry, pharmacology, contemporary application, and

toxicology. Biomed Research International 2014:1-31

Bautista DM, Movahed P, Hinman A, Axelsson HE, Sterner O, Högestätt ED, Julius D, Jordt S-E, Zygmunt PM (2005) Pungent products from garlic activate the sensory ion channel TRPA1. Proc Natl Acad Sci U S A 102:12248–12252 Available at: http://www.pubmedcentral.nih.gov/articlerender.fcgi?artid=1189336&tool=pmcentrez&rendertype=abstract.

Bautista DM, Siemens J, Glazer JM, Tsuruda PR, Basbaum AI, Stucky CL, Jordt S-E, Julius D (2007) The menthol receptor TRPM8 is the principal detector of environmental cold. Nature 448:204–208.

Braz JM, Nassar MA, Wood JN, Basbaum AI (2005) Parallel "pain" pathways arise from subpopulations of primary afferent nociceptor. Neuron 47:787–793 Available at: http://www.ncbi.nlm.nih.gov/pubmed/16157274 [Accessed July 23, 2014].

Caspani O, Heppenstall P a (2009) TRPA1 and cold transduction: an unresolved issue? J Gen Physiol 133:245–249.

Colburn RW, Lubin M Lou, Stone DJ, Wang Y, Lawrence D, D'Andrea MR, Brandt MR, Liu Y, Flores CM, Qin N (2007) Attenuated cold sensitivity in TRPM8 null mice. Neuron 54:379–386.

Cox JJ, Reimann F, Nicholas AK, Thornton G, Roberts E, Springell K, Karbani G, Jafri H, Mannan J, Raashid Y, Al-gazali L, Hamamy H, Valente EM, Gorman S, Williams R, Mchale DP, Wood JN, Gribble FM, Woods CG (2006) An SCN9A channelopathy causes congenital inability to experience pain. Nature 444:3–7.

Deering-Rice CE, Romero EG, Shapiro D, Hughen RW, Light AR, Yost GS, Veranth JM, Reilly CA (2011) Electrophilic components of diesel exhaust particles (DEP) activate transient receptor potential ankyrin-1 (TRPA1): a probable mechanism of acute pulmonary toxicity for DEP. Chem Res Toxicol 24:950–959 Available at: http://www.pubmedcentral.nih.gov/articlerender.fcgi?artid=3133601&tool=pmcentrez&rendertype=abstract.

Dhaka A, Murray AN, Mathur J, Earley TJ, Petrus MJ, Patapoutian A (2007) TRPM8 is required for cold sensation in mice. Neuron 54:371–378 Available at: http://www.ncbi.nlm.nih.gov/pubmed/17481391 [Accessed October 10, 2013].

Dib-hajj SD, Geha P, Waxman SG (2017) Sodium channels in pain disorders : pathophysiology and prospects for treatment. PAIN 158:97-107.

Fajardo O, Meseguer V, Belmonte C, Viana F (2008) TRPA1 channels mediate cold temperature sensing in mammalian vagal sensory neurons: pharmacological and geneticevidence. J Neurosci 28:7863–7875.

Friedland K, Harteneck C (2017) Spices and odorants as TRP channel activators. In: Springer Handbook of Odor (Buettner A, ed), pp 85–86. Cham: Springer

International Publishing. Available at: http://dx.doi.org/10.1007/978-3-319-26932-0_34.

Gingras J, Smith S, Matson DJ, Johnson D, Nye K, Couture L, Feric E, Yin R, Moyer BD, Peterson ML, Rottman JB, Beiler RJ, Malmberg AB, Mcdonough SI (2014) Global Nav1 . 7 knockout mice recapitulate the phenotype of human congenital indifference to pain. Plos One 9(9):e105895.

Jordt S-E, Bautista DM, Chuang H-H, McKemy DD, Zygmunt PM, Högestätt ED, Meng ID, Julius D (2004) Mustard oils and cannabinoids excite sensory nerve fibres through the TRP channel ANKTM1. Nature 427:260–265.

Karashima Y, Talavera K, Everaerts W, Janssens A, Kwan KY, Vennekens R, Nilius B, Voets T (2009) TRPA1 acts as a cold sensor in vitro and in vivo. Proc Natl Acad Sci U S A 106:1273–1278.

Kwan KY, Allchorne AJ, Vollrath M a, Christensen AP, Zhang D-S, Woolf CJ, Corey DP (2006) TRPA1 contributes to cold, mechanical, and chemical nociception but is not essential for hair-cell transduction. Neuron 50:277–289 Available at: http://www.ncbi.nlm.nih.gov/pubmed/16630838 [Accessed December 12, 2013].

Madrid R, de la Peña E, Donovan-Rodriguez T, Belmonte C, Viana F (2009) Variable threshold of trigeminal cold-thermosensitive neurons is determined by a balance between TRPM8 and Kv1 potassium channels. J Neurosci 29:3120–3131 Available at: http://www.ncbi.nlm.nih.gov/pubmed/19279249 [Accessed October 12, 2013].

McKemy DD (2005) How cold is it? TRPM8 and TRPA1 in the molecular logic of cold sensation. Mol Pain 1:16.

Moparthi L, Survery S, Kreir M, Simonsen C, Kjellbom P, Högestätt ED, Johanson U, Zygmunt PM (2014) Human TRPA1 is intrinsically cold- and chemosensitive with and without its N-terminal ankyrin repeat domain. Proc Natl Acad Sci U S A 111:16901–16906 Available at: http://www.ncbi.nlm.nih.gov/pubmed/25389312 [Accessed December 3, 2014].

Paper C (1999) Sodium channels and pain. PNAS 96:7635–7639.

Ran C, Hoon MA, Chen X (2016) The coding of cutaneous temperature in the spinal cord. Nat Publ Gr Available at: http://dx.doi.org/10.1038/nn.4350.

Roper SD (2014) TRPs in Taste and Chemesthesis. In: Mammalian Transient Receptor Potential (TRP) Cation Channels: Volume II (Nilius B, Flockerzi V, eds), pp 827–871.

Story GM, Peier AM, Reeve AJ, Eid SR, Mosbacher J, Hricik TR, Earley TJ, Hergarden AC, Andersson D a, Hwang SW, McIntyre P, Jegla T, Bevan S, Patapoutian A (2003) ANKTM1, a TRP-like channel expressed in nociceptive neurons, is activated by cold temperatures. Cell 112:819–829.

Teichert RW, Memon T, Aman JW, Olivera BM (2014) Using constellation pharmacology to define comprehensively a somatosensory neuronal subclass. Proc Natl Acad Sci U S A 111:2319–2324.

Venkatachalam K, Montell C (2007) TRP channels. Annu Rev Biochem 76:387–417 Available at: http://www.ncbi.nlm.nih.gov/pubmed/17579562 [Accessed September 23, 2013].

Vriens J, Nilius B, Voets T (2014) Peripheral thermosensation in mammals. Nat Rev Neurosci 15:573–589.

Waxman SG (2012) Sodium channels, the electrogenisome and the electrogenistat: lessons and questions from the clinic. J Physiol 590:2601–2612 Available at: http://www.pubmedcentral.nih.gov/articlerender.fcgi?artid=3424719&tool=pmcentrez&rendertype=abstract [Accessed November 24, 2013].

Weiss J, Pyrski M, Jacobi E, Bufe B, Willnecker V, Schick B, Zizzari P, Gossage SJ, Greer C a, Leinders-Zufall T, Woods CG, Wood JN, Zufall F (2011) Loss-of-function mutations in sodium channel Nav1.7 cause anosmia. Nature 472:186–190.

Yarmolinsky DA, Peng Y, Pogorzala LA, Rutlin M, Hoon MA, Zuker CS, Yarmolinsky DA, Peng Y, Pogorzala LA, Rutlin M, Hoon MA, Zuker CS (2016) Coding and Plasticity in the Mammalian Thermosensory System Article Coding and Plasticity in the Mammalian Thermosensory System. Neuron:1–14.

Zimmermann K, Leffler A, Babes A, Cendan CM, Carr RW, Kobayashi J, Nau C, Wood JN, Reeh PW (2007) Sensory neuron sodium channel Nav1.8 is essential for pain at low temperatures. Nature 447:855–858.

CHAPTER 2

COLD-SENSITIVITY OF TRPA1-EXPRESSING NEURONS

Published as:

Tosifa Memon, Kevin Chase, Lee S Leavitt, Baldomero M. Olivera and Russell W. Teichert (2017) TRPA1 expressing levels and excitability brake by K_V channels influence cold sensitivity of TRPA1-expressing neurons. *Neuroscience* 353: 76-86.

Neuroscience 353 (2017) 76–86

TRPA1 EXPRESSION LEVELS AND EXCITABILITY BRAKE BY K_V CHANNELS INFLUENCE COLD SENSITIVITY OF TRPA1-EXPRESSING NEURONS

TOSIFA MEMON, KEVIN CHASE, LEE S. LEAVITT, BALDOMERO M. OLIVERA AND RUSSELL W. TEICHERT*

Department of Biology, University of Utah, 257 S. 1400 E., Salt Lake City, UT 84112, United States

Abstract—The molecular sensor of innocuous (painless) cold sensation is well-established to be transient receptor potential cation channel, subfamily M, member 8 (TRPM8). However, the role of transient receptor potential cation channel, subfamily A, member 1 (TRPA1) in noxious (painful) cold sensation has been controversial. We find that TRPA1 channels contribute to the noxious cold sensitivity of mouse somatosensory neurons, independent of TRPM8 channels, and that TRPA1-expressing neurons are largely non-overlapping with TRPM8-expressing neurons in mouse dorsal-root ganglia (DRG). However, relatively few TRPA1-expressing neurons (e.g., responsive to allyl isothiocyanate or AITC, a selective TRPA1 agonist) respond overtly to cold temperature *in vitro*, unlike TRPM8-expressing neurons, which almost all respond to cold. Using somatosensory neurons from TRPM8−/− mice and subtype-selective blockers of TRPM8 and TRPA1 channels, we demonstrate that responses to cold temperatures from TRPA1-expressing neurons are mediated by TRPA1 channels. We also identify two factors that affect the cold-sensitivity of TRPA1-expressing neurons: (1) cold-sensitive AITC-sensitive neurons express relatively more TRPA1 transcripts than cold-insensitive AITC-sensitive neurons and (2) voltage-gated potassium (K_V) channels attenuate the cold-sensitivity of some TRPA1-expressing neurons. The combination of these two factors, combined with the relatively weak agonist-like activity of cold temperature on TRPA1 channels, partially explains why few TRPA1-expressing neurons respond to cold. Blocking K_V channels also reveals another subclass of noxious cold-sensitive DRG neurons that do not express TRPM8 or TRPA1 channels. Altogether, the results of this study provide novel insights into the cold-sensitivity of different subclasses of somatosensory neurons.

Key words: TRPA1, TRPM8, K_V1.2, cold pain, ion channel, pharmacology.

*Corresponding author.
E-mail address: russ.teichert@utah.edu (R. W. Teichert).

Abbreviations: AITC, allyl isothiocyanate; DRG, dorsal-root ganglia; FBS, fetal bovine serum; HEPES, 4-(2-Hydroxyethyl)piperazine-1-ethanesulfonic acid; K_V, voltage-gated potassium channel; ROI, region of interest; SNR, signal to noise; TRP, transient receptor potential channel.

http://dx.doi.org/10.1016/j.neuroscience.2017.04.001
0306-4522/

INTRODUCTION

Cold is analgesic when moderate (Proudfoot et al., 2006) and painful when extreme (Foulkes and Wood, 2007). These contradictory effects of cold in warm-blooded animals may be due to differences at the molecular, cellular, or circuit level (Vriens et al., 2014; Palkar et al., 2015; Lolignier et al., 2016). At the molecular level, temperature-sensitive transient receptor potential (thermoTRP) channels such as TRPM8 and TRPA1 have been reported to detect cold temperatures (Talavera et al., 2008). TRPM8, the first molecular sensor of cold-sensation, discovered in 2002, is widely accepted as a cold-sensor (Peier et al., 2002; Madrid et al., 2006; Bautista et al., 2007; Dhaka et al., 2007). TRPA1, on the other hand, was first characterized as a noxious cold-sensor (Story et al., 2003) but some follow-up studies were in conflict with this conclusion, resulting in an ongoing debate about the role of TRPA1 as a cold-sensor (Kwan et al., 2006; Bautista et al., 2007; Fajardo et al., 2008; Caspani and Heppenstall, 2009; Karashima et al., 2009; del Camino et al., 2010; Knowlton et al., 2010; Chen et al., 2013; Ran et al., 2016). Today, TRPA1 is accepted to have a role in pain and inflammation, but its involvement in cold sensation remains controversial.

This controversy encompasses numerous studies that address the issue at the molecular, cellular and behavioral levels (Kwan et al., 2006; Karashima et al., 2009; Cordero-morales et al., 2011; Miyake et al., 2016). One key observation that underlies this controversy is that only a small percentage of TRPA1-expressing somatosensory neurons respond overtly to noxious cold temperatures in neuronal cell culture (Babes et al., 2004; Jordt et al., 2004; Bautista et al., 2006; Fajardo et al., 2008; Karashima et al., 2009). Consistent with these studies, we also find that only a subset of TRPA1-expressing neurons respond to noxious cold stimuli. Even though the cold-sensitivity of TRPA1 channels has been studied at the molecular level (Sawada et al., 2007; Jabba et al., 2014; Miyake et al., 2016), it is difficult to explain why only a subset of the TRPA1-expressing neuronal population responds to cold. Therefore, to investigate why cold-sensitivity is not uniformly observed in TRPA1-expressing neurons, we have characterized this neuronal population to evaluate contributing factors.

Our data strongly suggest that cold responses in TRPA1-expressing neurons are mediated by TRPA1

channels without any contribution from TRPM8 channels. Further, to understand why only a subset of TRPA1-expressing neurons responds to cold, we hypothesized that additional factors, such as excitability brake by K_V channels and differences in TRPA1 expression levels among these neurons might influence cold-sensitivity of TRPA1-expressing neurons. Here, we present evidence that these two factors significantly contribute to the cold-sensitivity of TRPA1-expressing neurons.

EXPERIMENTAL PROCEDURES

Dissociated dorsal-root ganglia (DRG) cell cultures from WT and transgenic mice

Cell cultures were prepared from mouse Lumbar DRG at different ages, from postnatal day 3 (P3) to postnatal day 67 (P67). Mouse strains used for cell preparations were wild-type C57BL/6 mice, TRPM8−/− in a C57BL/6 genetic background (The Jackson Laboratory stock # 8198 (Bautista et al., 2007) and TRPA1−/− mice in a mixed genetic background (The Jackson Laboratory stock # 6401 (Kwan et al., 2006). All experimental results reported for a given mouse strain and age were obtained from three or more cell cultures prepared from different mice (in total ~30 mice), consisting of both sexes. All experiments conducted with mouse tissues were approved by the Institutional Animal Care and Use Committee (IACUC) of the University of Utah and were conducted in accordance with the National Institutes of Health guide for the care and use of Laboratory animals. Detailed descriptions of DRG cell preparations and calcium-imaging protocols were reported previously (Teichert et al., 2012a,b, 2014; Smith et al., 2013).

Briefly, lumbar DRG neurons were dissociated by treating DRGs with trypsin followed by mechanical trituration. Neurons were then plated into the center of a silicone ring that was previously attached to the floor of a 24-well poly-D-lysine coated plate. After allowing the cells to adhere to the floor of the plate for approximately 1 h, 1 mL of media was added to each well. The media (MEM + supplements) consisted of minimal essential media (MEM) (Invitrogen, Waltham, MA, USA) supplemented with 10% fetal bovine serum (FBS), 1× penicillin/streptomycin, 10 mM HEPES, and 0.4% (w/v) Glucose, pH 7.4. The plated cells were placed in a 5% CO_2 incubator at 37 °C overnight.

TRPA1 and TRPM8-expressing HEK cell lines

HEK293 cell-lines were kindly provided by Dr. Christopher Reilly (Department of Pharmacology and Toxicology, University of Utah, Salt Lake City, UT, USA) (Deering-Rice et al., 2011). Wild-type HEK293 cells were grown in DMEM:F12 supplemented with 5% FBS and 1× penicillin/streptomycin. HEK293 cell-lines stably overexpressing either human TRPM8 or TRPA1 channels were grown similarly with the addition of 300 μg/mL Geneticin as described previously (Deering-Rice et al., 2011). These cells were treated with trypsin and plated onto the 24-well poly-D-lysine coated plates in the same manner as the DRG cells and incubated overnight for calcium-imaging experiments.

Calcium-imaging experiments and pharmacology

For calcium-imaging experiments, neurons or HEK293 cells were incubated with Fura2-AM dye for 1 h at 37 °C and 0.5 h at room temperature. All the calcium-imaging experiments were carried out at room-temperature, except when cold bath solutions were used as stimuli. Single distinct cells were visually identified in the field of view and defined as a region of interest (ROI). For each ROI, a calcium-imaging trace was generated with the standard 340 nm/380 nm ratio as the *y*-axis and time in minutes as the *x*-axis. Data points were captured every two or three seconds. The fluorescence of 340 nm/380 nm excitation ratio (510 nm emission) indicates the relative level of intracellular calcium in the neuron or cell. All the stimuli indicated by arrows in each figure were applied for 15 s before washout. Horizontal bars, cold ramp, and triangles in some figures indicate longer incubation times, including 30-second applications of 4 °C (triangles), 2-min applications of 4 °C (cold ramp) and longer incubations with pharmacological agents (horizontal bars), including the TRPM8 blocker, M8-B (Almeida et al., 2012), the TRPA1 blocker, HC-030031 (Eid et al., 2008), and the $K_V1.2$ blocker, κM-conotoxin RIIIJ (Teichert et al., 2014). Cold bath solutions were placed in an ice bucket and applied either manually for 30 s or circulated using a peristaltic pump for 2 min, as described in each figure legend. Temperature was monitored by placing a thermocoupler in the experimental well, close to the imaging field of view. To differentiate between neuronal and non-neuronal populations of DRG cells, a depolarizing pulse of 30 mM extracellular potassium, $[K^+]_o$, was applied at the beginning of each experiment.

Calcium-imaging experiments were carried out with DRG observation solution consisting of 145 mM NaCl, 5 mM KCl, 2 mM $CaCl_2$, 1 mM $MgCl_2$, 1 mM sodium citrate, 10 mM HEPES, and 10 mM glucose, pH 7.4. For $[K^+]_o$ application, 30 mM K^+ was made by increasing the concentration of KCl and reducing the concentration of NaCl in DRG observation solution without affecting the osmolarity. All pharmacological agents, including menthol, allyl isothiocyanate (AITC), M8-B, and HC-030031, were purchased from Sigma–Aldrich (except κM-conotoxin RIIIJ). Working concentrations were made in DRG Observation solution from respective stock solutions. Stock solutions were 640 mM menthol in ethanol, 10.2 M AITC oil, 1 mM M8-B and 30 mM HC-030031 in DMSO, and 10 μM κM-conotoxin RIIIJ in DRG Observation solution. For all experiments, the isomer of menthol used was (1R,2S,5R)-(−)-menthol.

Single-cell RT-qPCR

Immediately following calcium-imaging experiments, individual neurons of interest were harvested with patch pipettes (~3 μm diameter) containing recombinant RNAse Inhibitor (Invitrogen, Waltham, MA, USA). After collecting each cell in a patch pipette tip, the pipette tip

was broken into a PCR tube to transfer the neuronal cell body to a ten microliter solution containing 10% Triton X-100 and SuperScript IV VILO Master Mix (Invitrogen, Waltham, MA, USA) for reverse transcription. The mRNA in each sample was reverse transcribed at 50 °C for 10 min. The ten microliter reverse transcription (RT) reaction was then divided into two different PCR reactions containing either TRPA1 primers or β-actin primers. TRPA1 primer pairs 5′-AGGTGATTTTTAAAA CATTGCTGAG-3′ and 5′-CTCGATAATTGATGTCTCC TAGCAT-3′ yield cDNA fragments of 168 bp, and β-actin primer pairs 5′-GGCCCAGAGCAAGAGAGG TATCC-3′ and 5′-ACGCACGATTTCCCTCTCAGC-3′ yield cDNA fragments of 460 bp (Kwan et al., 2006). Both TRPA1 and β-actin primer pairs span an intron and yield DNA fragments amplified from genomic DNA of 500 bp and 914 bp, respectively. For real-time PCR, the cDNA from RT reaction (4 μL) was denatured at 95 °C, annealed at 60 °C, and extended at 72 °C for 40 cycles with 10 μL KAPA SYBR FAST qPCR MM (Kapa Biosystems, Wilmington, MA, USA) and 400 nM of TRPA1 or 250 nM of β-actin primers in 20 μL PCR reactions. Control samples included cells with no AITC response or extracellular DRG observation solution. Only the cells with β-actin signal were included in the analysis. For data analysis, ΔCq and relative quantities of TRPA1 cDNA molecules in individual cells were determined by normalizing the Cq value of each cell to the Cq cutoff of 34 for TRPA1 reactions (Ståhlberg et al., 2013). Cq cutoff and efficiency of reactions was estimated from a standard curve of RNA isolated from mouse DRG neurons. Finally, 2% agarose gel and melt curves were used to confirm the specificity of the end product.

Data analysis and statistics

For calcium-imaging experiments, cells were defined as ROIs using the 10× brightfield image. Traces are shown in figures as ratiometric values for each ROI in the series of images taken at two- or three-second intervals over the time-frame of the experiment. Ratiometric values are indicators of relative cytosolic calcium levels. The time-course of the ratio was analyzed using a set of functions written in R (www.r-project.org). The maldiquant package (Gibb and Strimmer, 2012) was used to correct baselines, smooth, and detect peaks. All traces were baseline corrected using the estimateBaseline function with the "SNIP" method and smoothed using the smoothIntensity function with the "SavitzkyGolay" method and a halfWindowSize of 3. Peaks were detected using the detectPeaks function with the "MAD" method, a halfWindowSize of 30 and a SNR.lim setting of 4. All ROIs were scored as yes/no (binary) response to each input based on the presence of a peak in the response window region. Thresholds were established to define possible peaks in time windows of probable response to the given inputs. We used a signal-to-noise (SNR) threshold of 4 and a value above baseline threshold of 0.05. These threshold values give a false positive rate < 0.001 (e.g. peaks during times of no input). Traces with obvious abnormal response patterns were removed from the analysis.

The percentage or frequency of cells responsive to a given stimulus or compound was determined using binary scoring described above. Also, to count the frequency of neuronal responders in DRG cultures, only the cells responding to $[K^+]_o$ were included in the analysis. The frequency of responses was calculated for

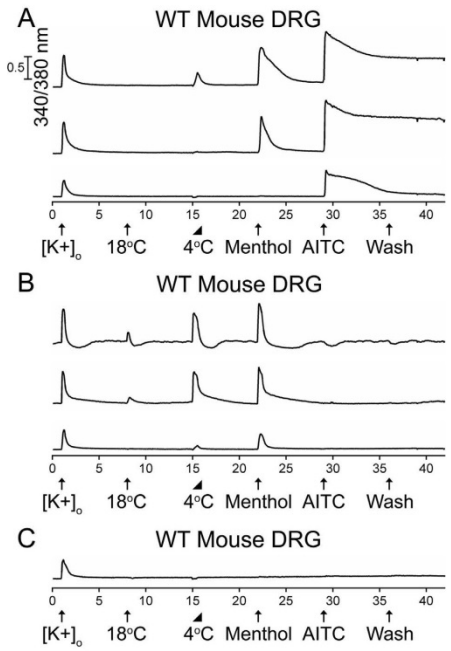

Fig. 1. The diversity of neuronal responses from adult (> Postnatal day 45) wild-type mouse DRG to cold, menthol, and AITC. The units of the *x*-axis are minutes and the units of the *y*-axis are the 340/380 nm calcium-imaging ratio described in Materials and Methods. Calibration bar of 0.5 for 340/380 values applies to all the traces. The experimental protocol is depicted below the *x*-axis. Physiological or pharmacological challenges were administered at 7-min intervals. Abbreviations are as follows: $[K+]_o$, 30 mM $[K^+]_o$; 18 °C or 4 °C, bath solution at the respective temperature; Menthol, 400 μM menthol; AITC, 100 μM AITC; wash, replacement of static bath solution with identical bath solution. Arrows represent the 15-s application of each challenge. The triangle indicates a 30-s application of 4 °C solution, where the temperature was allowed to gradually rise in the well at room temperature. The aforementioned facts apply to subsequent figures also. (A) Representative traces from AITC-sensitive DRG neurons. A subset of DRG neurons responded to cold, menthol and AITC (2.9% ± 0.4%). Another subset responded to menthol and AITC (7.2% ± 0.7%). An additional subset only responded to AITC (26.5% ± 1.2%). See summary in Table 2. (B) Representative traces from menthol-sensitive and AITC-insensitive DRG neurons. A subset of DRG neurons responded to 18 °C and 4 °C bath applications, and menthol (5.3% ± 0.6%). Another subset only responded to 4 °C and menthol (2.4% ± 0.4%). See summary in Table 2. (C) Representative trace from a large subset of DRG neurons that did not respond to cold, menthol or AITC. Percentage values refer to percentage of $[K+]_o$-responsive neurons (n = 1465) from 6 experimental trials from 3 mice.

each experimental trial and averaged for each culture. Mean frequencies across multiple cultures were determined for each set of experimental conditions. The mantelhaen.test function of R was used to perform a Cochran–Mantel–Haenszel chi-squared test (Agresti, 1990) for equality of response type frequency between mouse lines. The woolf test (Woolf, 1955) was used to test for heterogeneity between wells. The cor.test function in R was used to test for significant correlation between dCq and AITC response area. The t.test function in R was used to test for significant differences between dCq values in AITC+ and AITC− neuron populations.

RESULTS

Diverse response profiles observed among cold-sensitive DRG neurons

We used Fura-2 calcium imaging of dissociated adult mouse DRG neurons, coupled with various types of physiological and pharmacological challenges, to identify and characterize different neuronal subclasses. Fig. 1 illustrates the diversity of response phenotypes elicited by a depolarizing stimulus (30 mM extracellular K^+), cold temperatures (18 °C and 4 °C), menthol and AITC in DRG neurons (n = 1465) from wild-type C57BL/6 mice. Notably, a subset of the AITC-sensitive neurons responded to a 30-s application of noxious cold temperature (4 °C) and menthol (Fig. 1A). However, these represented a small minority (7.9% ± 1.2%) of the AITC-sensitive DRG neurons (A+ in Table 1). A larger subset (19.4% ± 1.7%) of AITC-sensitive neurons responded to menthol, but not to cold temperatures (Fig. 1A, Table 1). An additional subset (71.7% ± 1.9%) of AITC-sensitive DRG neurons responded only to AITC, without robust responses either to cold or menthol (Fig. 1A, Table 1). In contrast to the AITC-sensitive neurons, we observed that a large subset (67.8% ± 4.4%) of menthol-sensitive but AITC-insensitive (M+A− in Table 1) DRG neurons responded to innocuous cool temperatures (e.g. 18 °C, Fig. 1B, Table 1). However, a subset (30.4% ± 4.3%) of these neurons only responded to noxious cold temperatures (e.g. 4 °C, Fig. 1B, Table 1). A large subset of DRG neurons did not respond to cold, menthol or AITC, but did respond to a depolarizing stimulus, which activated voltage-gated calcium channels, eliciting a calcium influx (Fig. 1C). Distributions of these functional response phenotypes as percentages of the total neuronal cell population (K^+) have been listed in Table 2.

Cold responses in AITC-sensitive neurons depend on TRPA1 and not TRPM8 channels

The experiment illustrated in Fig. 1 employed DRG neurons from wild-type mice. We repeated this experimental protocol multiple times with DRG neurons from TRPA1−/− mice and TRPM8−/− mice (Fig. 2). Using DRG neurons from TRPA1−/− mice (n = 1107), we observed all of the functional phenotypes shown in Fig. 1B (see Fig. 2B, Tables 1 and 2), but none of the functional phenotypes exhibited in Fig. 1A. These neurons apparently all express TRPM8 channels and not TRPA1 channels because they responded to menthol (a TRPM8 agonist), but not to AITC (a TRPA1 agonist). Using DRG neurons from TRPM8−/− mice (n = 1535), we did not observe any of the functional phenotypes shown in Fig. 1B and we continued to observe all of the functional phenotypes shown in

Table 1. Response phenotypes as percentages of AITC+ (TRPA1-expressing) and Menthol+, AITC− (TRPM8-expressing) mouse DRG neurons or HEK cells

	WT Mice		TRPM8−/−Mice		TRPA1 HEK cells	
	% A+ (n = 541)	SEM	% A+ (n = 478)	SEM	% A+ (n = 494)	SEM
4°+M+A+	7.9%	1.2%	6.7%	1.1%	47.2%	2.2%
4°−M+A+	19.4%	1.7%	31.4%	2.1%	34.0%	2.1%
4°−M−A+	71.7%	1.9%	60.7%	2.2%	14.8%	1.6%
4°+M−A+	0.9%	0.4%	1.3%	0.5%	4.0%	0.9%
Total A+ cells	100.0%		100.0%		100.0%	
	WT Mice		TRPA1−/−Mice		TRPM8 HEK cells	
	% M+A− (n = 115)	SEM	% M+A− (n = 74)	SEM	% M+A− (n = 880)	SEM
18°+4°+M+A−	67.8%	4.4%	*47.3%	5.8%	89.8%	1.0%
18°−4°+M+A−	30.4%	4.3%	*40.5%	5.7%	9.2%	1.0%
18°−4°−M+A−	1.7%	1.2%	*12.2%	3.8%	1.0%	0.3%
Total M+A− cells	100.0%		100.0%		100.0%	

Examples of response phenotypes are shown in Figs. 1, 2 and 5.

Abbreviations are the following: 18°, 18° C for 15 s; 4°, 4° C for 30-s; M, Menthol; A, AITC; +, responsive; −, not responsive; n, number of cells; SEM, standard error of the mean.

The percentages in the table were calculated from the following:

WT Mice: 6 experimental trials from 3 cell cultures (mice).

TRPM8−/− mice: 7 experimental trials from 4 cell cultures (mice).

TRPA1−/− mice: 8 experimental trials from 3 cell cultures (mice).

TRPA1 HEK cells: 3 experimental trials from 3 cell cultures.

TRPM8 HEK cells: 4 experimental trials from 3 cell cultures.

*We observed significant differences in the frequency of each response phenotype between WT and TRPA1−/− mice. In general, the M+A− neurons from TRPA1−/− mice appear to have a higher cold-response threshold than M+A− neurons from WT mice. However, we did not investigate that observation further in this study.

Table 2. Response phenotypes of AITC+ (TRPA1-expressing) and Menthol+, AITC− (TRPM8-expressing) mouse DRG neurons as percentages of the total neuronal cell population

	WT Mice		TRPM8−/−Mice	
	% K^+ (n = 1465)	SEM	% K^+ (n = 1535)	SEM
4°+M+A+	2.9%	0.4%	2.1%	0.4%
4°−M+A+	7.2%	0.7%	9.8%	0.8%
4°−M−A+	26.5%	1.2%	18.9%	1.0%
4°+M−A+	0.3%	0.2%	0.4%	0.2%
Other neurons	63.1%	1.3%	68.9%	1.2%
Total neurons	100.0%		100.0%	
	WT Mice		TRPA1−/−Mice	
	% K^+ (n = 1465)	SEM	% K^+ (n = 1107)	SEM
18°+4°+M+A−	5.3%	0.6%	3.2%	0.5%
18°−4°+M+A−	2.4%	0.4%	2.7%	0.5%
18°−4°−M+A−	0.1%	0.1%	0.8%	0.3%
Other neurons	92.2%	0.7%	93.3%	0.8%
Total neurons	100.0%		100.0%	

Examples of response phenotypes are shown in Figs. 1, 2 and 5.
Abbreviations are the following: 18°, 18° C for 15 s; 4°, 4° C for 30 s; M, Menthol; A, AITC; +, responsive; −, not responsive; n, number of cells; SEM, standard error of the mean.
The percentages in the table were calculated from the following:
WT Mice: 6 experimental trials from 3 cell cultures (mice).
TRPM8−/− mice: 7 experimental trials from 4 cell cultures (mice).
TRPA1−/− mice: 8 experimental trials from 3 cell cultures (mice).

Fig. 1A (see Fig. 2A, Tables 1 and 2). We had previously attributed the menthol responses to TRPM8 channels in AITC-sensitive neurons (Teichert et al., 2012a) as menthol was considered a selective agonist of TRPM8 channels (Bautista et al., 2007) and shown to block mouse TRPA1 channels at high concentrations (Karashima et al., 2007; Xiao et al., 2008). However, our results from adult TRPM8−/− mice suggested that the responses to cold and menthol in AITC-sensitive neurons may be solely mediated by TRPA1 channels and not TRPM8 channels. This is consistent with previous studies that used similar concentrations of menthol and reported activation of TRPA1 channels in sensory neurons (Fajardo et al., 2008; Meseguer et al., 2008; Karashima et al., 2009). Furthermore, these results with TRPM8−/− mice suggested that TRPA1 and TRPM8 channels may be expressed in separate, non-overlapping DRG neuronal subclasses.

To further test these hypotheses, we utilized subtype-selective antagonists of TRPA1 and TRPM8 channels to block the responses to cold, menthol and AITC in wild-type adult mouse DRG neurons. Fig. 3A demonstrates that a selective antagonist of TRPA1 channels, HC-030031 (Eid et al., 2008), completely blocked the responses to cold, menthol and AITC in 96.9% ± 0.7% of the TRPA1-expressing (AITC sensitive) DRG neurons (n = 422), but did not block the cold and menthol responses in the TRPM8-expressing DRG neurons (menthol-sensitive but AITC insensitive). In the remaining ~3% of TRPA1-expressing neurons, HC-030031 blocked responses to cold, menthol and AITC by 88.9% ± 6.2%. Fig. 3B demonstrates that a selective antagonist of TRPM8 channels, M8-B (Almeida et al., 2012), completely blocked the responses to cold and menthol in 95.0% ± 2.9% of the TRPM8-expressing DRG neurons (n = 40), but did not block the cold and menthol responses in the TRPA1-expressing DRG neurons (AITC sensitive). In the remaining ~5% of TRPM8-expressing neurons, M8-B blocked responses to cold and menthol by 92.5% ± 4%. In addition to the results obtained from TRPA1−/− and TRPM8−/− mice, these results confirm that responses to cold and menthol in TRPA1-expressing DRG neurons (AITC sensitive) are solely mediated by TRPA1 channels. Moreover, TRPA1-mediated cold and menthol responses become evident in adult mice compared to neonates as the frequency of AITC-responsive (TRPA1-expressing) neurons increases with age (Fig. 4).

K_V1.2 channel blocker increases TRPA1-dependent cold responses

It is presently unclear what circumstances or states allow TRPA1 channels to be activated by noxious cold temperature, as only a small fraction of the TRPA1-expressing neurons or HEK cells (Fig. 5, Table 1) responded to a 30-s application of noxious cold temperature in our hands. However, by increasing the duration of the cold bath application (4 °C) from 30 s to 2 min, we observed a significant increase in cold responsiveness from approximately 8% to 24% of TRPA1-expressing mouse DRG neurons and from approximately 47% to 88% of human TRPA1-expressing HEK cells (Table 3). Additionally, in the presence of an antagonist of K_V1.2 channels, κM-conotoxin RIIIJ (RIIIJ), the percentage of TRPA1-expressing DRG neurons that responded to a 2-min application of 4 °C bath solution increased from approximately 24% to 49%, and responses to cold temperature in the absence of RIIIJ were amplified in the presence of RIIIJ (Fig. 6 and Table 3), suggesting that high expression of certain voltage-gated potassium (K_V) channels (including but not limited to K_V1.2) may blunt the response to cold in

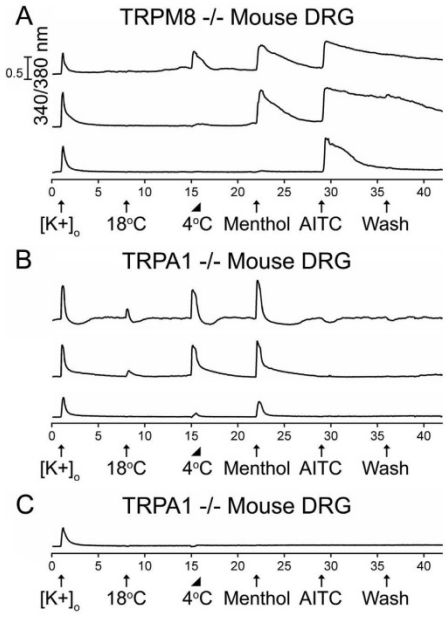

Fig. 2. The diversity of neuronal responses to cold, menthol, and AITC from (A) adult TRPM8−/− mouse DRG and (B & C) TRPA1−/− mouse DRG. The experimental protocol is identical to that described in the Fig. 1 legend. (A) AITC-sensitive DRG neurons that express TRPA1 channels were observed from TRPM8−/− mice. A subset of DRG neurons responded to cold, menthol and AITC (2.1% ± 0.4%). Another subset responded to menthol and AITC (9.8% ± 0.8%). An additional subset only responded to AITC (18.9% ± 1.0%). See summary in Table 2. (B) Menthol-sensitive DRG neurons that express TRPM8 channels were observed from TRPA1−/− mice. A subset of DRG neurons responded to 18 °C and 4 °C bath applications, and menthol (3.2% ± 0.5%). Another subset only responded to 4 °C and menthol (2.7% ± 0.5%). See summary in Table 2. (C) Representative trace from a large subset of DRG neurons that did not respond to cold, menthol or AITC. In this case, the trace is from a DRG neuron from a TRPA1−/− mouse. Percentage values refer to percentage of $[K+]_o$-responsive neurons (n = 1535 for TRPM8−/− and n = 1107 for TRPA1−/−) from 4 TRPM8−/− and 3 TRPA1−/− mice.

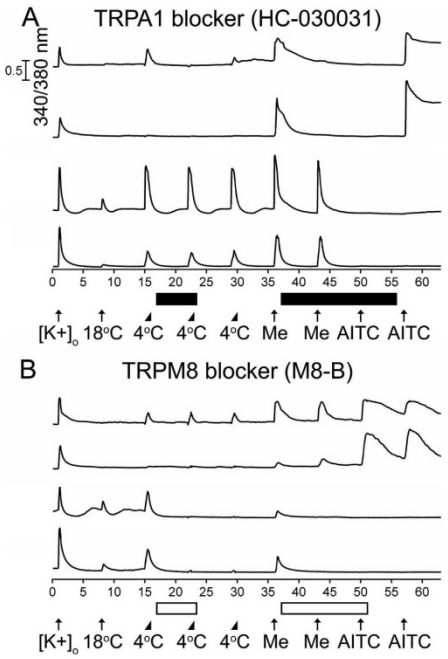

Fig. 3. Distribution of TRPA1 and TRPM8 channels in cold-, menthol- and AITC-sensitive adult mouse DRG neurons. The experimental protocol is similar to the protocol outlined in the Fig. 1 legend, with a few exceptions described below. Me is an abbreviation for 400 μM Menthol. (A) The TRPA1 antagonist HC-030031 (30 μM) selectively and completely blocked responses to cold, menthol, and AITC in 96.9% ± 0.7% of AITC-sensitive neurons (n = 422). The black horizontal bars indicate when HC-030031 was present in the bath solution. (B) The TRPM8 antagonist M8-B (1 μM) selectively and completely blocked responses to cold and menthol in 95.0% ± 2.9% of menthol-sensitive and AITC-insensitive neurons (n = 40). The open horizontal bars indicate when M8-B was present in the bath solution.

TRPA1-expressing neurons to a subthreshold level. These experiments with RIIIJ were conducted using neurons from TRPM8−/− mice (n = 2313) to demonstrate that the additional responses obtained in the presence of RIIIJ were mediated by TRPA1 channels and not TRPM8 channels (Fig. 6). Furthermore, the large majority of these cold responses were completely blocked by the TRPA1 channel blocker, HC-030031 (Fig. 6).

K_V1.2 blocker increases TRPM8- and TRPA1-independent cold responses

In addition to TRPM8- and TRPA1-expressing cold sensitive neurons, there are noxious cold-sensitive neurons that do not express TRPM8 or TRPA1 channels (Babes et al., 2004; Munns et al., 2007; Ran et al., 2016). We have observed that approximately 7% ± 2% of DRG neurons (n = 3364) that did not respond to menthol or AITC in fact responded to a 2-min cold-ramp to 4 °C (CS M−A− neurons). Interestingly, removal of an excitability brake by K_V channels that contain K_V1.2 subunits increased the frequency of CS M−A− neurons to approximately 12% ± 1% (Fig. 7). The molecular identity of such cold responses remains unknown.

TRPA1 expression levels influence cold-sensitivity of TRPA1-expressing neurons

Another factor that could contribute to the cold sensitivity of TRPA1-expressing neurons is functional expression of TRPA1 channels. We have observed that cold-sensitive AITC-sensitive (CS A+) neurons usually exhibit greater menthol and AITC responses than cold-insensitive

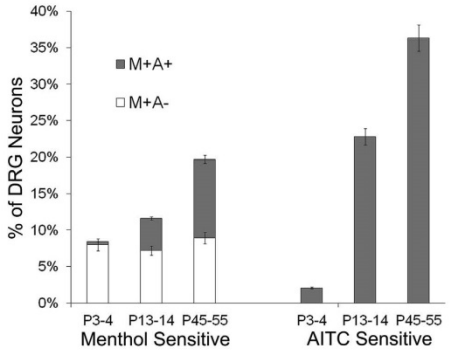

Fig. 4. Percentages of lumbar DRG neurons from wild-type mice at different ages that responded to menthol or AITC. At postnatal day 3 or 4 (P3-4), a very low percentage of neurons responded to AITC and nearly all of the menthol-sensitive neurons were insensitive to AITC. The menthol-responsive and AITC-non-responsive (M+A−) neurons, as a percentage of the neuronal cell population, remained relatively constant across different ages of mice. However, the AITC-sensitive neurons increased dramatically as a percentage of the neuronal cell population during postnatal development. Accordingly, the menthol-sensitive neurons that were also AITC sensitive (M+A+ neurons) increased as a percentage of the neuronal cell population during postnatal development. The legend shown above the stacked bar graphs for menthol-sensitive neurons only applies to the menthol-sensitive neurons. For each age of mice, at least 6 experimental trials were conducted, using at least 3 independently prepared cell cultures from different mice. Total number of neurons scored for each age category was 1412 for P3-4, 1385 for P13-14, and 1465 for P45-55. Error bars are ± SEM.

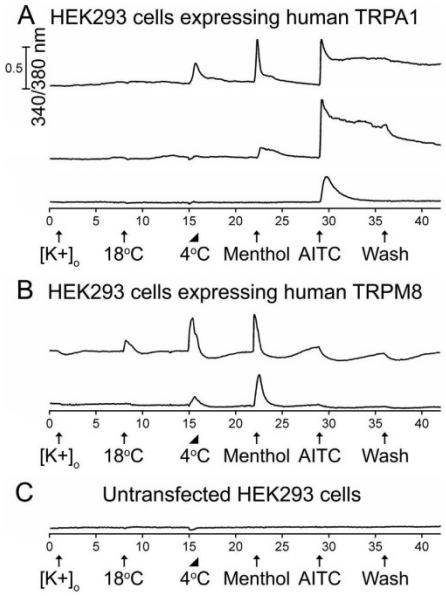

Fig. 5. The diversity of cold, menthol, and AITC responses from HEK293 cells stably expressing either human TRPA1 or TRPM8 channels. The experimental protocol is identical to that described in the Fig. 1 legend. (A) Representative traces from human TRPA1-expressing HEK cells. A subset responded to cold, menthol and AITC (47.2% ± 2.2%). Another subset responded to menthol and AITC (34.0% ± 2.1%). An additional subset only responded to AITC (14.8% ± 1.6%). See summary in Table 1. (B) Representative traces from human TRPM8-expressing HEK cells. A subset of these neurons responded to 18 °C and 4 °C bath applications, and menthol (89.8% ± 1.0%). Another subset only responded to 4 °C and menthol (9.2% ± 1.0%). See summary in Table 1. (C) Representative trace from untransfected HEK cells.

AITC-sensitive (Cl A+) neurons (e.g., AITC responses measured by peak height and time for cytosolic calcium to return to baseline, Fig. 1). Therefore, we hypothesized that CS A+ neurons may express more TRPA1 than Cl A+ neurons. To test this hypothesis, we performed single-cell RT-qPCR on cells of interest and determined relative quantities (RQ) of TRPA1 cDNA molecules in CS A+ and Cl A+ neurons. Indeed, we find that CS A+ neurons expressed, on an average, ~2.7-fold more TRPA1 transcripts, as compared to Cl A+ neurons (Fig. 8A). Furthermore, ΔCq of TRPA1 in each neuron positively correlated with AITC-elicited Ca^{2+} responses (Fig. 8B). Most of the neurons that did not respond to AITC also did not have any detectable TRPA1 transcripts but had β-actin transcripts (Fig. 8C), and samples without cells (no-template controls) did not have transcripts of either TRPA1 or β-actin (Fig. 8C). Lastly, the expected size of TRPA1 (~168 bp) and β-Actin (~460 bp) transcripts was confirmed by gel electrophoresis as shown in Fig. 8C. Hence, functional expression levels of TRPA1 channels also play an important role in determining whether a response to cold reaches threshold for detection in TRPA1-expressing neurons.

DISCUSSION

The experimental results obtained with DRG neurons from TRPA1−/− mice, TRPM8−/− mice, and wild-type mice, using selective antagonists of TRPA1 and TRPM8 channels, as well as HEK293 cells stably expressing human TRPA1 or TRPM8 channels, cumulatively indicate that responses to cold, menthol and AITC in TRPA1-expressing cells are all mediated by TRPA1 channels. Our finding is consistent with previous reports of TRPA1-dependent cold- and menthol-responses in sensory neurons of trigeminal ganglia (Karashima et al., 2009) and nodose ganglia (Fajardo et al., 2008). Our results also indicate that TRPA1 channels and TRPM8 channels are predominantly expressed in different, largely non-overlapping subsets of mouse DRG neurons, a conclusion that is also supported by recent single-cell RNA sequencing studies of mouse DRG neurons (Usoskin et al., 2014; Li et al., 2015). Therefore, the clear implication of the results is that TRPA1 channels, independent of TRPM8 channels, play a role in the detection of noxious-cold stimuli. In this paper, we have also demonstrated that expression levels of TRPA1 channels and K_V channels (including those that contain K_V1.2 subunits) are among

Table 3. Frequency of cold-responses from TRPA1-expressing mouse DRG neurons and HEK293 cells stably expressing human TRPA1 for different treatment conditions

Treatment	% AITC-responsive Mouse DRG neurons	% HEK293 cells stably expressing human TRPA1
4 °C (30 s)	7.9 ± 1.2% (n = 541)	47.2 ± 2.2% (n = 494)
4 °C (2 min)	24.0 ± 3.6% (n = 1171)	88.3 ± 2.6% (n = 894)
4 °C + RIIIJ (2 min)	48.5 ± 3.2% (n = 1171)	–

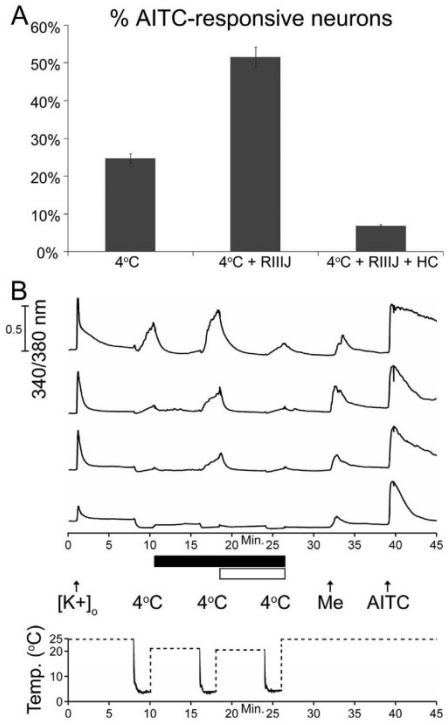

Fig. 6. The frequency of responses to cold increased in TRPA1-expressing (AITC responsive) DRG neurons from TRPM8−/− mice when potassium channels that contain $K_V1.2$ subunits were blocked by κM-conotoxin RIIIJ (RIIIJ). Mouse DRG neurons that responded to AITC (n = 796) were challenged with a 4 °C bath solution for 2-min prior to six-minute incubation with 1 μM RIIIJ and then again after incubation with RIIIJ in the continued presence of RIIIJ (black bar). The 2-min cold ramp was then repeated again in the presence of RIIIJ and the TRPA1 blocker, HC030031 (white bar). (A) The bar graph shows the percentage of AITC-responsive neurons that also responded to the 4 °C bath solution, 4 °C in the presence of RIIIJ, and 4 °C in the presence of RIIIJ and HC030031. (B) Representative calcium imaging traces and experimental protocol used to obtain the data in A. In these experiments, the bath solution was cooled to a temperature of 4 °C for 2 min, according to the temperature ramp shown on the time-scale of the x-axis. The temperature was monitored with a thermocoupler in the bath near the imaging field of view. Dashed lines indicate times when temperature data were not monitored in the bath because the bath solution was replaced by the room-temperature solution.

the factors that determine whether a TRPA1-expressing neuron responds overtly to noxious cold temperatures in calcium-imaging assays.

In a prior study, we identified putative cold thermosensors, such as those shown in Figs. 1B and 2B (which respond to innocuous cold temperatures), and correctly concluded that those neurons express TRPM8 channels, but not TRPA1 channels, because they responded to the application of menthol but not to AITC. However, we also identified putative cold nociceptors (which respond to noxious cold temperatures, but not innocuous cold temperatures), such as those shown in Figs. 1A and 2A, but incorrectly concluded that those neurons express both TRPM8 and TRPA1 channels because they responded to both menthol and AITC (Teichert et al., 2012a). However, in this study, we demonstrate conclusively that responses to cold, menthol and AITC are all mediated by TRPA1 channels in the putative cold nociceptors shown in Figs. 1A and 2A.

In the same prior study, we demonstrated that the putative cold nociceptors which express TRPA1 channels (see Figs. 1A and 2A) also co-express the voltage-gated Na^+ channel, $Na_V1.8$ (Teichert et al.,

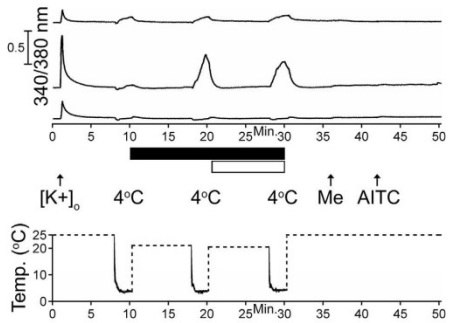

Fig. 7. Representative traces of cold-sensitive menthol- and AITC-unresponsive (CS M-A-) neurons. The experimental protocol shown below traces is similar to the protocol in Fig. 6, where the cold ramp was applied for 2 min with and without κM-RIIIJ, a selective blocker of $K_V1.2$ containing channels (black bar), and HC-030031, a TRPA1 blocker (white bar). About 7% ± 2% of K^+-responsive neurons (n = 3364) that were unresponsive to menthol or AITC responded to a 2-min cold ramp to 4 °C as illustrated by the top trace. In the presence of κM-RIIIJ, the frequency of CS M-A- neurons increased to approximately 12% ± 1% of DRG neurons, as shown in the middle trace, while the majority of menthol- and AITC-unresponsive neurons remained unaffected as shown in the bottom trace. The temperature was monitored with a thermocoupler in the bath near the imaging field of view. Dashed lines indicate times when temperature data were not monitored in the bath because the bath solution was replaced by the room-temperature solution.

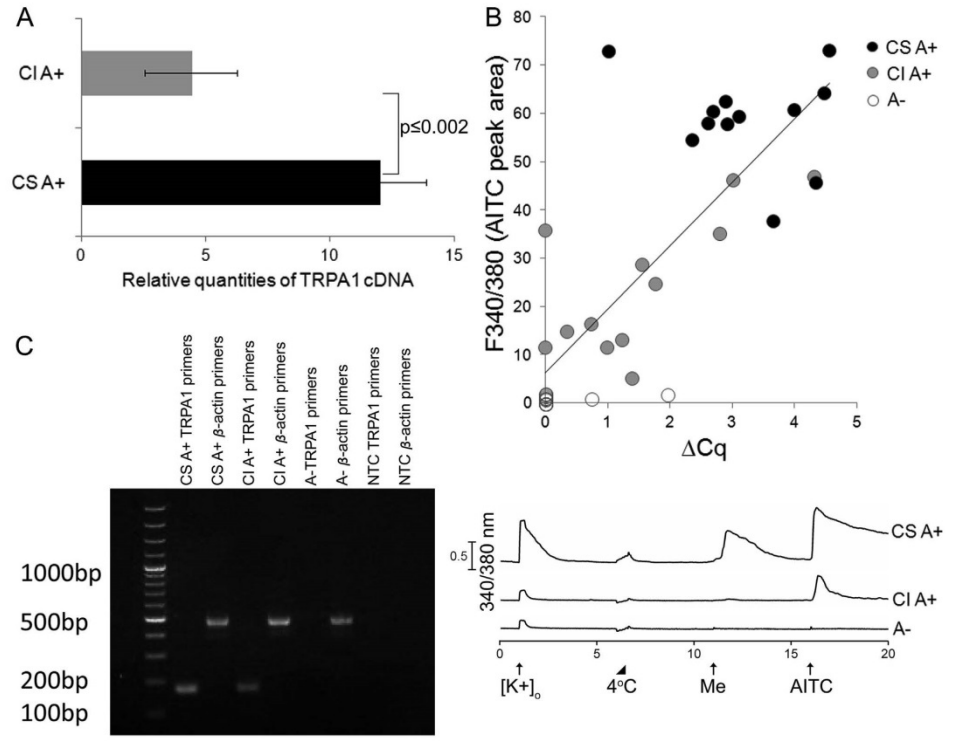

Fig. 8. Single-cell RT-qPCR for TRPA1 transcript levels. (A) Relative quantities of TRPA1 cDNA molecules for cold-sensitive AITC-responsive (CS A+) and cold-insensitive AITC-responsive (CI A+) neurons were determined for comparison (CS A+ , n = 12; CI A+ , n = 12; p-value = 0.002 by Welch's Two Sample t test). (B) AITC-elicited Ca^{2+} responses (peak area over 4-min) obtained from calcium imaging experiments positively correlated with ΔCq of TRPA1 for each neuronal cell. This dataset includes CS A+ (black circle, n = 12), CI A+ (gray circle, n = 12), and AITC-unresponsive neurons abbreviated A- (white circle, n = 12). Comparing ΔCq values with AITC response area in the entire data set, there exists a strong correlation (Pearson correlation = 0.81, p-value = 2.943e-09). (C) Representative gel image on left showing end product of single-cell RT-qPCR for cells (CS A+ , CI A+ , A-) and no cell (NTC) samples with calcium imaging response profile shown on right. Expected size of cDNA fragments for TRPA1 was ~168 bp and for β-actin was ~460 bp.

2012a), which has been shown to be essential for the sensation of cold pain (Zimmermann et al., 2007), but the low-threshold cold-thermosensor neurons (see Figs. 1B and 2B) did not express $Na_V1.8$ (Teichert et al., 2012a). Cumulatively, these data support a role for TRPA1 channels in the sensation of cold-induced pain.

Cold appears to be a weaker agonist of TRPA1 channels than menthol and AITC, which is reflected in the magnitude and frequency of cold responses in AITC-sensitive neurons and TRPA1-expressing HEK cells (Figs. 1A, 2A, 3A, 5A and Tables 1 and 2). Cold temperature elicits overt responses (above threshold) in AITC-sensitive (CS A+) neurons that express more TRPA1 transcripts than CI A+ neurons (Fig. 8). Others have hypothesized that TRPA1 expression levels may contribute to observed differences in cold sensitivity among TRPA1-expressing neurons (Karashima et al., 2009). In this study, we have demonstrated it empirically. Moreover, our findings are consistent with previous reports that claim cold-temperature is a weaker and slower activator of TRPA1 channels at the molecular level (Sawada et al., 2007; Karashima et al., 2009).

The weak and slow activation of TRPA1 by cold in some AITC-sensitive neurons can further be blunted by the presence of K_V channels to a sub-threshold level for detection (Fig. 6). K_V channels are known to blunt TRPM8-mediated cold responses (Madrid et al., 2009; Teichert et al., 2014) but their contribution to the cold-sensitivity of TRPA1-expressing neurons has not been reported previously. Hence, the combination of relatively low TRPA1 expression levels, relatively high K_V-channel expression levels and the relatively weak activation of TRPA1 channels by cold temperatures (compared to AITC) largely explain why most TRPA1-expressing neurons do not respond overtly to cold in calcium-imaging assays.

Even though our results support the hypothesis that TRPA1 channels are activated by cold temperatures, our data do not rule out the possibilities of indirect activation or sensitization of the TRPA1 channels by increases in reactive oxygen species (ROS) and intracellular calcium that may be elicited by cold temperatures (Zurborg et al., 2007; Andersson et al., 2008; del Camino et al., 2010; Miyake et al., 2016). These molecular mechanistic details are beyond the scope of our study but have been addressed elsewhere (Karashima et al., 2009; Moparthi et al., 2014; Miyake et al., 2016). Hence, the cold-sensitivity of TRPA1-expressing neurons is complex and dependent on multiple factors.

The significance of these contributing factors is not just limited to the normal physiology of cold-sensation but extends to its pathophysiology such as cold-allodynia and hypersensitivity. There is an increase in TRPA1 expression and reduction in K_V channel expression during cold-allodynia (Descoeur et al., 2011; Zhao et al., 2012). Also, ROS formation and cytokine release during and following an injury can further sensitize TRPA1 channels, resulting in cold-hypersensitivity (McNamara et al., 2007; del Camino et al., 2010; Bautista et al., 2013; Eberhardt et al., 2014). It is possible that the combination of these mechanisms results in the pain caused by cold via TRPA1. Therefore, therapy for cold-induced neuropathic pain may benefit by targeting multiple mechanisms, including TRPA1 channels and K_V channels.

FUNDING

This work was supported by the National Institute of General Medical Sciences Grant GM48677.

Acknowledgments—We are grateful to Dr. Rocio K. Finol-Urdaneta for initial training and continuous advice with single-cell RT-qPCR. We thank Dr. Christopher A. Reilly and Dr. Cassandra Rice, Department of Pharmacology and Toxicology, University of Utah, for providing us the HEK293 cell lines that stably express either TRPM8 or TRPA1 channels and for helpful suggestions regarding our manuscript. We thank Dr. Jean Rivier for peptide synthesis of κM-conotoxin RIIIJ, and My Huynh for assistance in preparing figures.

REFERENCES

Agresti A (1990) Categorical data analysis. New York, Wiley 11:230–235.

Andersson DA, Gentry C, Moss S, Bevan S (2008) Transient receptor potential A1 is a sensory receptor for multiple products of oxidative stress. J Neurosci 28:2485–2494.

Babes A, Zorzon D, Reid G (2004) Two populations of cold-sensitive neurons in rat dorsal root ganglia and their modulation by nerve growth factor. Eur J Neurosci 20:2276–2282.

Bautista DM, Jordt S-E, Nikai T, Tsuruda PR, Read AJ, Poblete J, Yamoah EN, Basbaum AI, Julius D (2006) TRPA1 mediates the inflammatory actions of environmental irritants and proalgesic agents. Cell 124:1269–1282.

Bautista DM, Siemens J, Glazer JM, Tsuruda PR, Basbaum AI, Stucky CL, Jordt S-E, Julius D (2007) The menthol receptor TRPM8 is the principal detector of environmental cold. Nature 448:204–208.

Bautista DM, Pellegrino M, Tsunozaki M (2013) TRPA1: a gatekeeper for inflammation. Annu Rev Physiol 75:181–200.

Caspani O, Heppenstall PA (2009) TRPA1 and cold transduction: an unresolved issue? J Gen Physiol 133:245–249.

Chen J, Kang D, Xu J, Lake M, Hogan JO, Sun C, Walter K, Yao B, Kim D (2013) Species differences and molecular determinant of TRPA1 cold sensitivity. Nat Commun 4:2501.

Cordero-morales JF, Gracheva EO, Julius D (2011) Cytoplasmic ankyrin repeats of transient receptor potential A1 (TRPA1) dictate sensitivity to thermal and chemical stimuli. Proc Natl Acad Sci U S A 108:1184–1191.

Deering-Rice CE, Romero EG, Shapiro D, Hughen RW, Light AR, Yost GS, Veranth JM, Reilly Ca (2011) Electrophilic components of diesel exhaust particles (DEP) activate transient receptor potential ankyrin-1 (TRPA1): a probable mechanism of acute pulmonary toxicity for DEP. Chem Res Toxicol 24:950–959.

del Camino D, Murphy S, Heiry M, Barrett LB, Earley TJ, Cook Ca, Petrus MJ, Zhao M, D'Amours M, Deering N, Brenner GJ, Costigan M, Hayward NJ, Chong JA, Fanger CM, Woolf CJ, Patapoutian A, Moran MM (2010) TRPA1 contributes to cold hypersensitivity. J Neurosci 30:15165–15174.

Descoeur J, Pereira V, Pizzocaro A, Francois A, Ling B, Maffre V, Couette B, Busserolles J, Courteix C, Noel J, Lazdunski M, Eschalier A, Authier N, Bourinet E (2011) Oxaliplatin-induced cold hypersensitivity is due to remodelling of ion channel expression in nociceptors. EMBO Mol Med 3:266–278.

Dhaka A, Murray AN, Mathur J, Earley TJ, Petrus MJ, Patapoutian A (2007) TRPM8 is required for cold sensation in mice. Neuron 54:371–378.

Eberhardt M et al (2014) H2S and NO cooperatively regulate vascular tone by activating a neuroendocrine HNO-TRPA1-CGRP signalling pathway. Nat Commun 5:4381.

Eid SR, Crown ED, Moore EL, Liang HYA, Choong KC, Dima S, Henze DA, Kane SA, Urban MO (2008) HC-030031, a TRPA1 selective antagonist, attenuates inflammatory- and neuropathy-induced mechanical hypersensitivity. Mol Pain 4:48.

Fajardo O, Meseguer V, Belmonte C, Viana F (2008) TRPA1 channels mediate cold temperature sensing in mammalian vagal sensory neurons: pharmacological and genetic evidence. J Neurosci 28:7863–7875.

Foulkes T, Wood JN (2007) Mechanisms of cold pain. Channels:154–160.

Gibb S, Strimmer K (2012) MALDIquant: a versatile R package for the analysis of mass spectrometry data. Bioinformatics 28:2270–2271.

Jabba S, Goyal R, Sosa-Pagán JO, Moldenhauer H, Wu J, Kalmeta B, Bandell M, Latorre R, Patapoutian A, Grandl J (2014) Directionality of temperature activation in mouse TRPA1 ion channel can be inverted by single-point mutations in ankyrin repeat six. Neuron 82:1017–1031.

Jordt S, Bautista DM, Chuang H, Meng ID, Julius D (2004) Mustard oils and cannabinoids excite sensory nerve fibres through the TRP channel ANKTM1. Nature 427:260–265.

Karashima Y, Damann N, Prenen J, Talavera K, Segal A, Voets T, Nilius B (2007) Bimodal action of menthol on the transient receptor potential channel TRPA1. J Neurosci 27:9874–9884.

Karashima Y, Talavera K, Everaerts W, Janssens A, Kwan KY, Vennekens R, Nilius B, Voets T (2009) TRPA1 acts as a cold sensor in vitro and in vivo. Proc Natl Acad Sci U S A 106:1273–1278.

Knowlton WM, Bifolck-Fisher A, Bautista DM, McKemy DD (2010) TRPM8, but not TRPA1, is required for neural and behavioral responses to acute noxious cold temperatures and cold-mimetics in vivo. Pain 150:340–350.

Kwan KY, Allchorne AJ, Vollrath MA, Christensen AP, Zhang D-S, Woolf CJ, Corey DP (2006) TRPA1 contributes to cold, mechanical, and chemical nociception but is not essential for hair-cell transduction. Neuron 50:277–289.

Li C-L, Li K-C, Wu D, Chen Y, Luo H, Zhao J-R, Wang S-S, Sun M-M, Lu Y-J, Zhong Y-Q, Hu X-Y, Hou R, Zhou B-B, Bao L, Xiao H-S, Zhang X (2015) Somatosensory neuron types identified by high-

coverage single-cell RNA-sequencing and functional heterogeneity. Cell Res:1–20.
Lolignier XS, Gkika D, Andersson XD, Leipold E, Vetter XI, Viana F, Noël XJ, Busserolles XJ, Université C, Auvergne U (2016) New insight in cold pain: role of ion channels. Mod Clin Perspect 36:11435–11439.
Madrid R, Donovan-Rodriguez T, Meseguer V, Acosta MC, Belmonte C, Viana F (2006) Contribution of TRPM8 channels to cold transduction in primary sensory neurons and peripheral nerve terminals. J Neurosci 26:12512–12525.
Madrid R, de la Peña E, Donovan-Rodriguez T, Belmonte C, Viana F (2009) Variable threshold of trigeminal cold-thermosensitive neurons is determined by a balance between TRPM8 and Kv1 potassium channels. J Neurosci 29:3120–3131.
McNamara CR, Mandel-Brehm J, Bautista DM, Siemens J, Deranian KL, Zhao M, Hayward NJ, Chong Ja, Julius D, Moran MM, Fanger CM (2007) TRPA1 mediates formalin-induced pain. Proc Natl Acad Sci U S A 104:13525–13530.
Meseguer V, Karashima Y, Talavera K, D'Hoedt D, Donovan-Rodriguez T, Viana F, Nilius B, Voets T (2008) Transient receptor potential channels in sensory neurons are targets of the antimycotic agent clotrimazole. J Neurosci 28:576–586.
Miyake T, Nakamura S, Zhao M, So K, Inoue K, Numata T, Takahashi N, Shirakawa H, Mori Y, Nakagawa T, Kaneko S (2016) Cold sensitivity of TRPA1 is unveiled by the prolyl hydroxylation blockade-induced sensitization to ROS. Nat Commun 7:1–10.
Moparthi L, Survery S, Kreir M, Simonsen C, Kjellbom P, Högestätt ED, Johanson U, Zygmunt PM (2014) Human TRPA1 is intrinsically cold- and chemosensitive with and without its N-terminal ankyrin repeat domain. Proc Natl Acad Sci U S A 111:16901–16906.
Munns C, AlQatari M, Koltzenburg M (2007) Many cold sensitive peripheral neurons of the mouse do not express TRPM8 or TRPA1. Cell Calcium 41:331–342.
Palkar R, Lippoldt EK, McKemy DD (2015) The molecular and cellular basis of thermosensation in mammals. Curr Opin Neurobiol 34:14–19.
Peier AM, Moqrich A, Hergarden AC, Reeve AJ, Andersson DA, Story GM, Earley TJ, Dragoni I, McIntyre P, Bevan S, Patapoutian A (2002) A TRP channel that senses cold stimuli and menthol. Cell 108:705–715.
Proudfoot CJ, Garry EM, Cottrell DF, Rosie R, Anderson H, Robertson DC, Fleetwood-Walker SM, Mitchell R (2006) Analgesia mediated by the TRPM8 cold receptor in chronic neuropathic pain. Curr Biol 16:1591–1605.
Ran C, Hoon MA, Chen X (2016) The coding of cutaneous temperature in the spinal cord. Nat Neurosci 19:1201–1209.
Sawada Y, Hosokawa H, Hori A, Matsumura K, Kobayashi S (2007) Cold sensitivity of recombinant TRPA1 channels. Brain Res 1160:39–46.
Smith NJ, Hone AJ, Memon T, Bossi S, Smith TE, McIntosh JM, Olivera BM, Teichert RW (2013) Comparative functional expression of nAChR subtypes in rodent DRG neurons. Front Cell Neurosci 7:1–11.
Ståhlberg A, Rusnakova V, Forootan A, Anderova M, Kubista M (2013) RT-qPCR work-flow for single-cell data analysis. Methods 59:80–88.
Story GM, Peier AM, Reeve AJ, Eid SR, Mosbacher J, Hricik TR, Earley TJ, Hergarden AC, Andersson DA, Hwang SW, McIntyre P, Jegla T, Bevan S, Patapoutian A (2003) ANKTM1, a TRP-like channel expressed in nociceptive neurons, is activated by cold temperatures. Cell 112:819–829.
Talavera K, Nilius B, Voets T (2008) Neuronal TRP channels: thermometers, pathfinders and life-savers. Trends Neurosci 31:287–295.
Teichert RW, Raghuraman S, Memon T, Cox JL, Foulkes T, Rivier JE, Olivera BM (2012a) Characterization of two neuronal subclasses through constellation pharmacology. Proc Natl Acad Sci U S A 109:12758–12763.
Teichert RW, Smith NJ, Raghuraman S, Yoshikami D, Light AR, Olivera BM (2012b) Functional profiling of neurons through cellular neuropharmacology. Proc Natl Acad Sci U S A 109:1388–1395.
Teichert RW, Memon T, Aman JW, Olivera BM (2014) Using constellation pharmacology to define comprehensively a somatosensory neuronal subclass. Proc Natl Acad Sci U S A 111:2319–2324.
Usoskin D, Furlan A, Islam S, Abdo H, Lönnerberg P, Lou D, Hjerling-Leffler J, Haeggström J, Kharchenko O, Kharchenko PV, Linnarsson S, Ernfors P (2014) Unbiased classification of sensory neuron types by large-scale single-cell RNA sequencing. Nat Neurosci 18:145–153.
Vriens J, Nilius B, Voets T (2014) Peripheral thermosensation in mammals. Nat Rev Neurosci 15:573–589.
Woolf B (1955) On estimating the relation between blood group and disease. Ann Hum Genet 19:251–253.
Xiao B, Dubin AE, Bursulaya B, Viswanath V, Jegla TJ, Patapoutian A (2008) Identification of transmembrane domain 5 as a critical molecular determinant of menthol sensitivity in mammalian TRPA1. Channels 28:9640–9651.
Zhao M, Isami K, Nakamura S, Shirakawa H, Nakagawa T, Kaneko S (2012) Acute cold hypersensitivity characteristically induced by oxaliplatin is caused by the enhanced responsiveness of TRPA1 in mice. Mol Pain 8:55.
Zimmermann K, Leffler A, Babes A, Cendan CM, Carr RW, Kobayashi J, Nau C, Wood JN, Reeh PW (2007) Sensory neuron sodium channel Nav1.8 is essential for pain at low temperatures. Nature 447:855–858.
Zurborg S, Yurgionas B, Jira JA, Caspani O, Heppenstall PA (2007) Direct activation of the ion channel TRPA1 by Ca2+. Nat Neurosci 10:277–279.

(Received 6 January 2017, Accepted 1 April 2017)
(Available online 10 April 2017)

CHAPTER 3

FUNCTIONAL EXPRESSION OF VOLTAGE-GATED SODIUM CHANNELS IN TRPM8- AND TRPA1-EXPRESSING NEURONS

Section 3.2 published in:

Teichert RW, Raghuraman S, **Memon T**, Cox JL, Foulkes T, Rivier JE, Olivera BM (2012) Characterization of two neuronal subclasses through constellation pharmacology. Proc Natl Acad Sci U S A 109(31):12758-63

3.1 Background

TRPM8-expressing neurons can respond to a broad range of innocuous and noxious cold temperatures while a subset of TRPA1-expressing neurons sense cold temperatures only in the noxious range, e.g., below 15°C (Story et al., 2003; Dhaka et al., 2007; Teichert et al., 2012, 2014). If the activation of TRPM8 or TRPA1 channels in the nerve terminals in skin is to result in the sensation of cold temperatures, the activation of these channels must result in the propagation of action potentials in the axons of their respective neurons (Tracey, 2017). This requires the activation of TRPM8 or TRPA1 channels to be functionally coupled to voltage-gated sodium (Na_V) channels (Ogata and Ohishi, 2002; Catterall et al., 2005). Therefore, we studied the functional expression of Na_V channels in TRPM8- and TRPA1-expressing neurons using novel calcium-imaging based assays.

3.2 Distribution of $Na_V1.8$ Channel

The Na_V1 channel family is comprised of nine types of functional α subunits and 4 types of accessory β subunits (Catterall et al., 2005). The “pore-forming” α subunits of Na_V channels are divided into two major categories based on their block by tetrodotoxin (TTX) into TTX-sensitive (TTX-S) and TTX-resistant (TTX-R) subtypes. Five out of nine Na_V channel subunits are highly expressed in sensory neurons of DRG. Among these five subunits, $Na_V1.8$, a TTX-R channel, is essential for excitability of sensory neurons at noxious cold temperature (Zimmermann et al., 2007; Abrahamsen et al., 2008). Thus, we studied the distribution of $Na_V1.8$ channels in TRPM8- and TRPA1-expressing neurons to understand how these channels and neurons contribute to noxious

cold-sensation (Teichert et al., 2012).

3.2.1 Experimental Procedures

To determine the distribution of Na_V channel subunits in sensory neurons using calcium imaging, we used a similar approach described in Chapter 1. We identified TRPM8-expressing neurons by their responses to menthol and we identified TRPA1-expressing neurons by their responses to AITC. To identify sodium channel subtypes, we used a broad spectrum sodium channel activator, veratridine (V) (Farrag et al., 2008; Fekete et al., 2009), along with the depolarization by extracellular potassium (K). Neurons from adult (>45 days old) wild-type (WT) mice were briefly incubated with 30 μM veratridine (Enzo Life Sciences) for 2 minutes followed by a 15-second application of 15 mM potassium (Figure 3.1A). To determine the TTX-R component of veratridine, neurons were preincubated with 1μM TTX before and during veratridine treatment (Figure 3.1B). Similar experimental protocols were performed in adult $Na_V1.8$-/- mice to evaluate the contribution of $Na_V1.8$ to the TTX-R component of veratridine effects. Additionally, 1 μM of μO-MrVIB, a selective blocker of $Na_V1.8$ (Wilson et al., 2011), was used along with veratridine and TTX (Figure 3.2).

Response peak heights elicited by 15 mM K^+ before TTX and veratridine treatment (control) were averaged and compared to the K^+ response during the treatment (Teichert et al., 2012). Percentage change in response peak height during veratridine and TTX treatment was averaged for M+A- (TRPM8-expressing) and M+A+ (TRPA1-expressing) neurons. Table 3.1 compares the average response peak height as a percentage of control peak height across neuronal cell-types and multiple experimental conditions.

3.2.2 Results

Veratridine causes direct and indirect (i.e., amplification of the response to K^+ depolarization) responses in M+A- and M+A+ neurons (Figure 3.1A). In M+A- neurons, TTX completely blocked both direct and indirect effects of veratridine (Figure 3.1B) suggesting these neurons predominantly express TTX-S Na_V channels. In M+A+ neurons, TTX completely blocked only veratridine-elicited direct effects, suggesting that these neurons also express TTX-S Na_V channels. However, veratridine-elicited indirect effects were only partially blocked by TTX, as shown in Figure 3.1B. This indirect effect of veratridine in presence of TTX suggested the presence of TTX-R Na_V channels in M+A+ neurons. Therefore, we tested for the presence of TTX-R $Na_V1.8$ channel in M+A+ neurons using $Na_V1.8$-/- mice. Indeed, TTX completely blocked both veratridine-elicited direct and indirect effects in $Na_V1.8$-/- mice (Figure 3.2B, Table 3.1). To further confirm the presence of $Na_V1.8$ in M+A+ neurons in WT mice, we employed a selective blocker of $Na_V1.8$ channel, conopeptide μO-MrVIB. Again, 1 μM μO-MrVIB (co-applied with TTX) completely blocked the veratridine elicited indirect effects in M+A+ neurons of WT mice (Figure 3.2C, Table 3.1). Hence, our results with $Na_V1.8$-/- mice and μO-MrVIB convincingly show that M+A+ neurons express $Na_V1.8$ channels while M+A- neurons do not.

3.3 Distribution of TTX-S Na_V Channels

Calcium imaging experiments with veratridine suggested both M+A- and M+A+ neurons express TTX-S Na_V channels (Figure 3.1). However, the composition of these TTX-S Na_V channels remains unknown. Sensory neurons of DRG predominantly express

three TTX-S Na_V channel subtypes: $Na_V1.1$, $Na_V1.6$, and $Na_V1.7$ (Waxman, 2012; Zhang et al., 2013). Identifying specific TTX-S Na_V channel subtypes in these neuronal cell-types can give us a better insight into how information sensed by these neurons is processed.

Veratridine activates TTX-S Na_V channel subtypes more effectively than the TTX-R $Na_V1.8$ channel (Farrag et al., 2008). However, veratridine can induce a strong and irreversible increase in intracellular Ca^{2+}, limiting our ability to identify specific Na_V channel subtypes (Figure 3.1). Therefore, we employed another sodium channel activator, sea anemone toxin peptide ATXII, along with Na_V channel blockers, μ-conopeptides and TTX, to determine the distribution of TTX-S Na_V channels.

3.3.1 Experimental Procedures

ATXII binds extracellular side (site 3) of Na_V channels and activates (by delaying inactivation) these channels in a dose-dependent manner, being most potent on $Na_V1.1$ > $Na_V1.6$ > $Na_V1.7$ (Table 3.2) (Oliveira et al., 2004; Wanke et al., 2009; Snape et al., 2010). Therefore, we used different concentrations of ATXII (Alomone Labs) to selectively activate these channels starting with 100 nM to activate $Na_V1.1$, 1 μM to activate $Na_V1.6$, and 20 μM to activate $Na_V1.7$. Neurons were incubated with ATXII for 2 minutes followed by K^+ depolarization. ATXII-elicited amplification of K^+ depolarization was then subjected to the block by either conopeptide μ-TIIIA ($Na_V1.1$ blocker) or conopeptides μ-PIIIA/μ-GIIIA ($Na_V1.1$ and $Na_V1.6$ blocker) or TTX ($Na_V1.1$, $Na_V1.6$, and $Na_V1.7$ blocker) (Wilson et al., 2011; Zhang et al., 2013). We utilized the combination of ATXII and selective blockers to evaluate the functional expression of

TTX-S Na_V channel subtypes in sensory neurons, especially TRPM8 and TRPA1 expressing neurons.

Response peak height was measured for K+ depolarization before (control) and after ATXII treatment. Similarly, peak height of K depolarization during blocker treatment was measured. Peak height of all the subsequent K responses were normalized to that of control for each neuron and averaged for either TRPM8 (M+A-) or TRPA1 (A+) expressing neurons. These values ± SEM are presented in Figure 3.3B and 3.4B for each Na_V channel subtype-specific experimental protocol. Furthermore, previously published single-cell RNA sequencing data (Usoskin et al., 2014) were processed to validate our finding with calcium imaging. Neurons expressing TRPM8 and TRPA1 were extracted and average gene expression of individual Na_V channel subtype was determined in these neuronal cell-types (Figure 3.7). Thresholding method recommended by Usoskin *et al.* was used to determine the fraction of positive neurons (Usoskin et al., 2014).

3.3.2 Results

To determine functional expression of TTX-S Na_V channel subtypes in sensory neurons using calcium imaging, we evaluated one Na_V channel subtype at a time. ATXII activates $Na_V1.1$ most effectively with EC_{50} of 6 nM (Oliveira et al., 2004). Therefore, we used 100 nM ATXII to primarily activate $Na_V1.1$ channel subtype in sensory neurons, especially TRPM8 (M+A-)- and TRPA1 (A+)-expressing neurons. On average, ATXII caused robust amplification of K depolarization in TRPM8-expressing neurons but not in TRPA1-expressing neurons (Figure 3.3). ATXII elicited amplification was then subjected to $Na_V1.1$ selective blocker, μ-TIIIA (Lewis et al., 2007; Wilson et al., 2011; Zhang et

al., 2013). As shown in Figure 3.3, ATXII amplification was significantly blocked by 10 μM μ-TIIIA treatment in M+A- neurons whereas A+ neurons remained unaffected. This suggests that TRPM8-expressing neurons express $Na_V1.1$ while TRPA1-expressing neurons mostly do not.

To determine functional expression of $Na_V1.6$ channels using calcium imaging, we used 1 μM ATXII along with the $Na_V1.1$ blocker μ-TIIIA to selectively activate $Na_V1.6$ and minimize the contribution of $Na_V1.1$. In this case, ATXII-elicited amplification of K depolarization was subjected to the block by conopeptide μ-PIIIA, a selective blocker of both $Na_V1.1$ and $Na_V1.6$ (Wilson et al., 2011; Zhang et al., 2013). Therefore, any amplification in presence of ATXII and μ-TIIIA and subsequent block by μ-PIIIA is likely due to contribution of $Na_V1.6$. We find that even though 1 μM ATXII amplifies K depolarization in M+A- neurons, the block by μ-PIIIA is not significant (Figure 3.4). In A+ neurons, there is neither significant amplification by ATXII nor significant block by μ-PIIIA. As μ-PIIIA can also block voltage-gated potassium channel, K_V1, we performed similar experiments with conopeptide μ-GIIIA, which also blocks $Na_V1.1$ and $Na_V1.6$ without blocking K_V1 channels (Leipold et al., 2016). Again, preliminary experiments with μ-GIIIA (Figure 3.5) suggest that both TRPM8 and TRPA1 expressing neurons show very little expression of $Na_V1.6$.

Like $Na_V1.1$ and $Na_V1.6$, we are currently developing experimental protocols to determine functional expression of $Na_V1.7$ using calcium imaging. ATXII activates $Na_V1.7$ with EC_{50} of 1.8 μM (Oliveira et al., 2004). Therefore, we will use combination of 20 μM ATXII and conopeptide μ-GIIIA to selectively activate $Na_V1.7$ and minimize

the contribution of $Na_V1.1$ and $Na_V1.6$. The amplification of K depolarization in presence of ATXII and μ-GIIIA will further be subjected to block by TTX, blocker of $Na_V1.1$, $Na_V1.6$, and $Na_V1.7$. The amplification by ATXII in presence of μ-GIIIA and subsequent block by TTX will indicate presence of $Na_V1.7$ channels. Using this experimental protocol (Figure 3.6), we will determine the functional expression of $Na_V1.7$ in TRPM8- and TRPA1-expressing neurons. So far, preliminary experiments suggest that both of these distinct neuronal cell-types express $Na_V1.7$ (Figure 3.6).

3.4 Discussion

Based on calcium-imaging experiments, we find that most TRPM8- and TRPA1-expressing neurons express $Na_V1.7$ but do not express $Na_V1.6$ channels. Also, these two distinct neuronal cell-types differ from each other in their functional expression of $Na_V1.1$ and $Na_V1.8$ channels: TRPA1-expressing neurons co-express $Na_V1.8$ channels and TRPM8-expressing neurons co-express $Na_V1.1$ channels. These observations along with single-cell RNA sequencing data (Figure 3.7) suggest that TRPM8-expressing neurons predominantly express TTX-S $Na_V1.1$ and $Na_V1.7$ channels while TRPA1-expressing neurons predominantly express TTX-S $Na_V1.7$ and TTX-R $Na_V1.8$ channels.

Among five Na_V channel subtypes highly expressed in DRG neurons, we have determined functional expression of four subtypes, $Na_V1.1$, 1.6, 1.7, and 1.8. Another TTX-R Na_V channel, $Na_V1.9$, is highly expressed in TRPA1 expressing neurons but not in TRPM8 expressing neurons (Figure 3.7). $Na_V1.9$, like $Na_V1.8$, also plays an important role in painful cold-sensation (Dib-Hajj et al., 2015; Lolignier et al., 2015). Unfortunately, we currently lack pharmacological tools to determine the functional

expression of $Na_V1.9$ channel using calcium imaging. Thus, we will continue to use calcium imaging and screen natural products, especially venom components of cone snails, for discovery of $Na_V1.9$-selective activators and blockers (Terlau and Olivera, 2004; Teichert et al., 2015).

Co-expression of accessory β-subunits can modulate the activity and sensitivity of functional α-subunits of Na_V channels (Ogata and Ohishi, 2002; Catterall et al., 2005). Recently, Olivera and Yoshikami labs discovered a novel conopeptide, μO§-GVIIJ, that can discriminate among certain β-subunits of Na_V channels (Gajewiak et al., 2014). Therefore, using μO§-GVIIJ, we can now determine the functional expression of β-subunits in TRPM8- and TRPA1-expressing neurons. Furthermore, screening cone snail venom components using calcium imaging may also lead us to identify novel conopeptides to help discriminate not only α subunits but also β subunits of Nav channel subtypes in sensory neurons (Terlau and Olivera, 2004; Teichert et al., 2015).

Historically, Na_V channels are studied using electrophysiology. This high-precision technique has been useful in understanding the function and functional differences between Na_V channels (Armstrong, 1981; Ogata and Ohishi, 2002; Rush et al., 2007). But extracting high throughput information such as distribution of specific Na_V channel subtypes in multiple neuronal populations can be daunting with electrophysiology. Calcium imaging, on the other hand, has been useful in determining the functional expression of Na_V channel subtypes in multiple neuronal cell types simultaneously. Therefore, combining calcium imaging with electrophysiology in the future will help us understand how the functional coupling of specific Na_V channel subtypes with TRPA1 or

TRPM8 channels results in action potential firing in neurons where these channels are co-expressed (Waxman, 2012; Prescott et al., 2014).

3.5 References

Abrahamsen B, Zhao J, Asante CO, Cendan CM, Marsh S, Martinez-Barbera JP, Nassar M a, Dickenson AH, Wood JN (2008) The cell and molecular basis of mechanical, cold, and inflammatory pain. Science 321:702–705.

Armstrong CM (1981) Sodium channels and gating currents. Physiol Rev 61:644 LP-683 Available at: http://physrev.physiology.org/content/61/3/644.abstract.

Catterall WA, Goldin AL, Waxman SG (2005) Nomenclature and structure-function relationships of voltage-gated sodium channels. International Union of Pharmacology 57:397–409.

Dhaka A, Murray AN, Mathur J, Earley TJ, Petrus MJ, Patapoutian A (2007) TRPM8 is required for cold sensation in mice. Neuron 54:371–378 Available at: http://www.ncbi.nlm.nih.gov/pubmed/17481391 [Accessed October 10, 2013].

Dib-Hajj SD, Black J a., Waxman SG (2015) NaV1.9: a sodium channel linked to human pain. Nat Rev Neurosci 16:511–519.

Farrag KJ, Bhattacharjee A, Docherty RJ (2008) A comparison of the effects of veratridine on tetrodotoxin-sensitive and tetrodotoxin-resistant sodium channels in isolated rat dorsal root ganglion neurons. Pfl{ü}gers Arch - Eur J Physiol 455:929–938 Available at: http://dx.doi.org/10.1007/s00424-007-0365-5.

Fekete A, Franklin L, Ikemoto T, Rózsa B, Lendvai B, Sylvester Vizi E, Zelles T (2009) Mechanism of the persistent sodium current activator veratridine-evoked Ca elevation: implication for epilepsy. J Neurochem 111:745–756 Available at: http://www.ncbi.nlm.nih.gov/pubmed/19719824 [Accessed April 4, 2014].

Gajewiak J, Azam L, Imperial J, Walewska A, Green BR, Bandyopadhyay PK, Raghuraman S, Ueberheide B, Bern M, Zhou HM, Minassian N a, Hagan RH, Flinspach M, Liu Y, Bulaj G, Wickenden AD, Olivera BM, Yoshikami D, Zhang M-M (2014) A disulfide tether stabilizes the block of sodium channels by the conotoxin μO§-GVIIJ. Proc Natl Acad Sci U S A 111:2758–2763 Available at: http://www.pubmedcentral.nih.gov/articlerender.fcgi?artid=3932919&tool=pmcentrez&rendertype=abstract [Accessed October 15, 2014].

Leipold E, Ullrich F, Thiele M, Tietze AA, Terlau H, Imhof D, Heinemann SH (2016) Subtype-specific block of voltage-gated K+ channels by mu-conopeptides. Biochem

Biophys Res Commun 482(4):1135-1140.

Lewis RJ, Schroeder CI, Ekberg J, Nielsen KJ, Loughnan M, Thomas L, Adams DA, Drinkwater R, Adams DJ, Alewood PF (2007) Isolation and structure-activity of μ-conotoxin TIIIA , a potent inhibitor of tetrodotoxin-sensitive voltage-gated sodium channels. Mol Pharm 71:676–685.

Lolignier S, Bonnet C, Gaudioso C, Noël J, Ruel J, Amsalem M, Ferrier J, Rodat-Despoix L, Bouvier V, Aissouni Y, Prival L, Chapuy E, Padilla F, Eschalier A, Delmas P, Busserolles J (2015) The Nav1.9 channel is a key determinant of cold pain sensation and cold allodynia. Cell Rep 11:1067–1078 Available at: http://linkinghub.elsevier.com/retrieve/pii/S2211124715004143.

Ogata N, Ohishi Y (2002) Molecular diversity of structure and function of the voltage-gated Na+ channels. Jpn J Pharmacol 88:365–377.

Oliveira JS, Redaelli E, Zaharenko AJ, Cassulini RR, Konno K, Pimenta DC, Freitas JC, Clare JJ, Wanke E (2004) Binding specificity of sea anemone toxins to Nav 1.1-1.6 sodium channels: unexpected contributions from differences in the IV/S3-S4 outer loop. J Biol Chem 279:33323–33335.

Prescott S, Ma Q, De Koninck Y (2014) Normal and abnormal coding of somatosensory stimuli causing pain. Nat Neurosci 17:183–191.

Rush AM, Cummins TR, Waxman SG (2007) Multiple sodium channels and their roles in electrogenesis within dorsal root ganglion neurons. J Physiol 579:1–14.

Snape A, Pittaway JF, Baker MD (2010) Excitability parameters and sensitivity to anemone toxin ATX-II in rat small diameter primary sensory neurones discriminated by Griffonia simplicifolia isolectin IB4. J Physiol 588:125–137 Available at: http://www.pubmedcentral.nih.gov/articlerender.fcgi?artid=2821554&tool=pmcentrez&rendertype=abstract [Accessed November 24, 2013].

Story GM, Peier AM, Reeve AJ, Eid SR, Mosbacher J, Hricik TR, Earley TJ, Hergarden AC, Andersson D a, Hwang SW, McIntyre P, Jegla T, Bevan S, Patapoutian A (2003) ANKTM1, a TRP-like channel expressed in nociceptive neurons, is activated by cold temperatures. Cell 112:819–829.

Teichert RW, Memon T, Aman JW, Olivera BM (2014) Using constellation pharmacology to define comprehensively a somatosensory neuronal subclass. Proc Natl Acad Sci U S A 111:2319–2324.

Teichert RW, Raghuraman S, Memon T, Cox JL, Foulkes T, Rivier JE, Olivera BM (2012) Characterization of two neuronal subclasses through constellation pharmacology. Proc Natl Acad Sci U S A 109(31):12758-63.

Teichert RW, Schmidt EW, Olivera BM (2015) Constellation pharmacology : a new

paradigm for drug discovery. Annu Rev Pharmacol Toxicol 55:573-589.

Terlau H, Olivera BM (2004) Conus venoms: a rich source of novel ion channel-targeted peptides. Physiol Rev 84(1):41-68.

Tracey WD (2017) Nociception. Curr Biol 27:129–133.

Usoskin D, Furlan A, Islam S, Abdo H, Lönnerberg P, Lou D, Hjerling-Leffler J, Haeggström J, Kharchenko O, Kharchenko P V, Linnarsson S, Ernfors P (2014) Unbiased classification of sensory neuron types by large-scale single-cell RNA sequencing. Nat Neurosci 18:145-153.

Wanke E, Zaharenko AJ, Redaelli E, Schiavon E (2009) Actions of sea anemone type 1 neurotoxins on voltage-gated sodium channel isoforms. Toxicon 54:1102–1111 Available at: http://www.ncbi.nlm.nih.gov/pubmed/19393679 [Accessed November 24, 2013].

Waxman SG (2012) Sodium channels, the electrogenisome and the electrogenistat: lessons and questions from the clinic. J Physiol 590:2601–2612 Available at: http://www.pubmedcentral.nih.gov/articlerender.fcgi?artid=3424719&tool=pmcentrez&rendertype=abstract [Accessed November 24, 2013].

Wilson MJ, Yoshikami D, Azam L, Gajewiak J, Olivera BM, Bulaj G (2011) μ -Conotoxins that differentially block sodium channels NaV1.1 through 1 . 8 identify those responsible for action potentials in sciatic nerve. PNAS 108(25):10302-10307.

Zhang M-M, Wilson MJ, Gajewiak J, Rivier JE, Bulaj G, Olivera BM, Yoshikami D (2013) Pharmacological fractionation of tetrodotoxin-sensitive sodium currents in rat dorsal root ganglion neurons by μ-conotoxins. Br J Pharmacol 169:102–114.

Zimmermann K, Leffler A, Babes A, Cendan CM, Carr RW, Kobayashi J, Nau C, Wood JN, Reeh PW (2007) Sensory neuron sodium channel Nav1.8 is essential for pain at low temperatures. Nature 447:855–858.

Table 3.1: Average peak height as percentage of control in the presence of 30 μM Veratridine and 1 μM TTX

	M+A+ neurons	M+A– neurons
WT Mice	271 ± 16% (56 cells)	81 ± 10% (15 cells)
$Na_V1.8^{-/-}$ mice	76 ± 12% (58 cells)	69 ± 9% (10 cells)
WT Mice + 1 μM μO-MrVIB	76 ± 4% (74 cells)	54 ± 6% (19 cells)

Each average ± SEM is from ≥ four independent trials.

Table 3.2: Affinities of ATXII and μ-conopeptides for Na_V channel subtypes

Affinities of Peptides		Na_V 1.1	Na_V 1.6	Na_V 1.7
EC_{50} (μM) of ATXII*		0.006	0.240	1.8
IC_{50} or K_d (μM) of μ-conopeptides**	μ-TIIIA	0.9	25	>100
	μ-PIIIA	0.12	0.1	>100
	μ-GIIIA	0.26	0.68	>100

*Adapted from Oliveira et al., 2004 & Wanke et al., 2009
**Adapted from Wilson et al., 2011

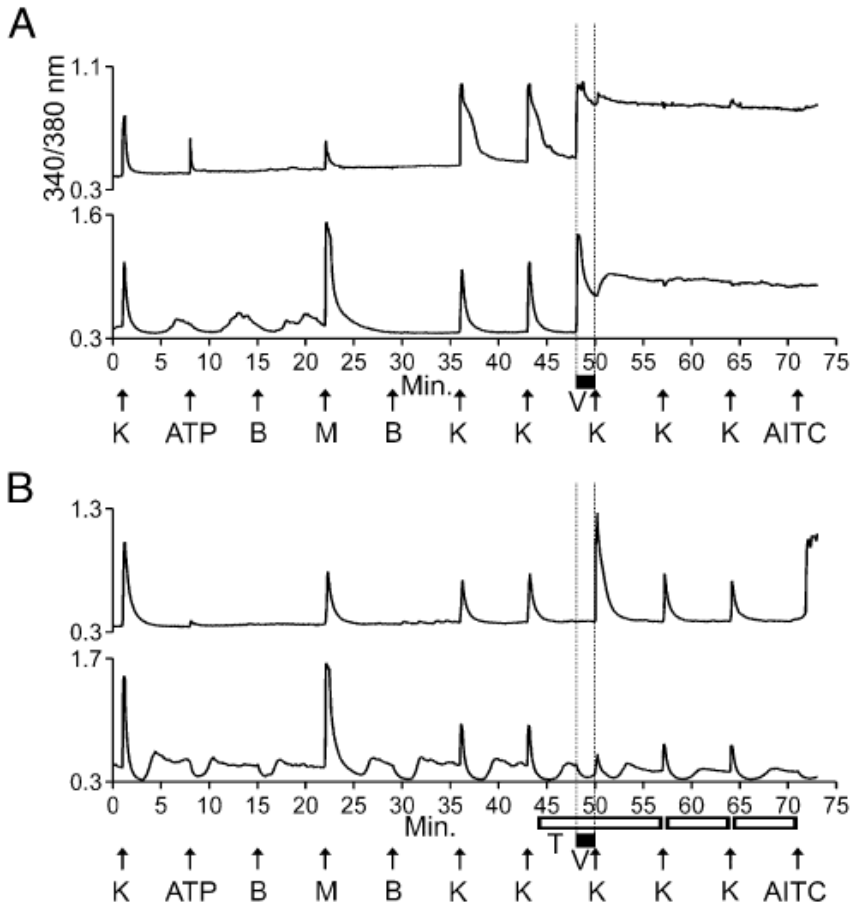

Figure 3. 1: Veratridine-elicited responses were blocked by TTX in both M+A- and M+A+ neurons. However, in the presence of both TTX and veratridine, KCl-elicited responses were amplified in M+A+ neurons but were blocked in M+A- neurons. The vertical dashed lines are for clarity only, indicating when 30 μM veratridine was present in the well. (A) Both M+A- and M+A+ neurons responded immediately to application of veratridine (black bar) with an elevated and sustained increase in [Ca^{2+}]. Here, "K" indicates 20 mM KCl. (B) The immediate responses to veratridine shown between the vertical dashed lines in A were blocked by 1 μM TTX (open horizontal bars) in both M+A- and M+A+ neurons. However, in the presence of both TTX and veratridine, KCl-elicited responses were amplified in M+A+ neurons (Upper) but were partially blocked in M+A- neurons (Lower). After application of veratridine and TTX, the average KCl-elicited response as a percentage of control peak height was 271 ± 16% for M+A+ cells (n = 6 trials, 15 cells total). Here, "K" indicates 25 mM KCl at minute 1 and then 15 mM KCl at subsequent time points (15 mM KCl was used because it made the amplification observed in the upper trace of B more evident, while the block observed in the lower trace of B remained clear) (Teichert et al., 2012).

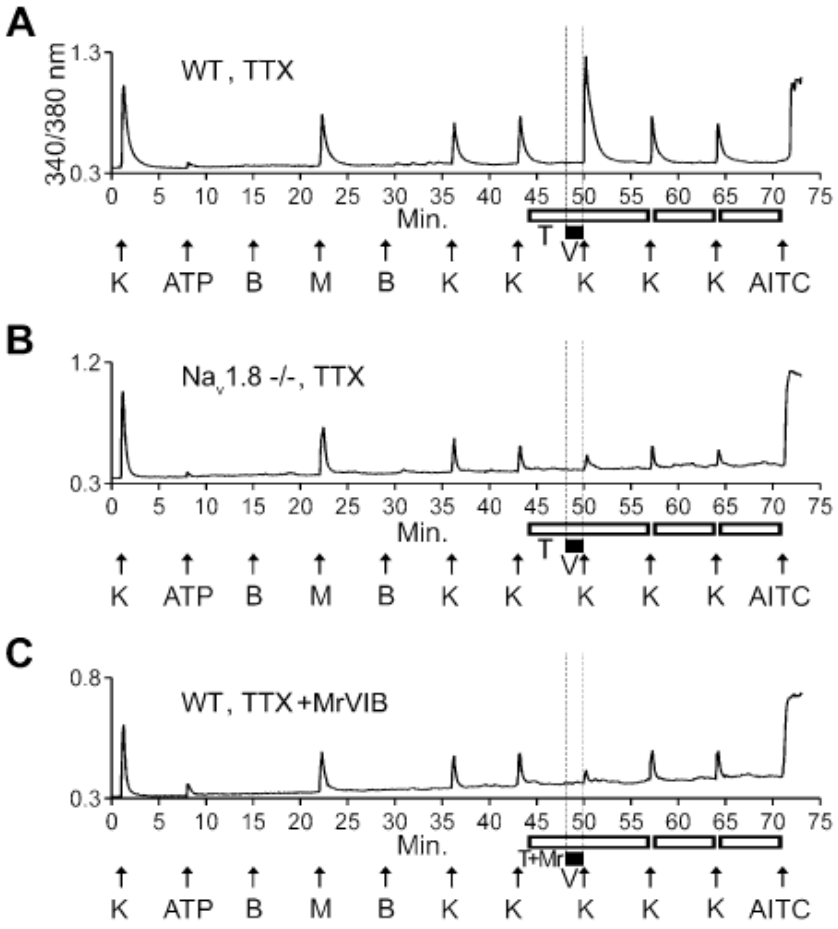

Figure 3.2: In the presence of TTX and veratridine, KCl-elicited responses were amplified in M+A+ neurons in WT (A) but were blocked in $Na_V1.8$-/- mice (B). In WT mice, the KCl-elicited responses also were blocked when both 1 μM TTX and 1 μM μO-MrVIB were coapplied with 30 μM veratridine (C). The vertical dashed lines are for clarity only, to indicate when veratridine was present in the well. The experimental protocol shown in Figure 3.1 was used to obtain these traces, with the exception of μO-MrVIB also was used in C (Teichert et al., 2012).

A.

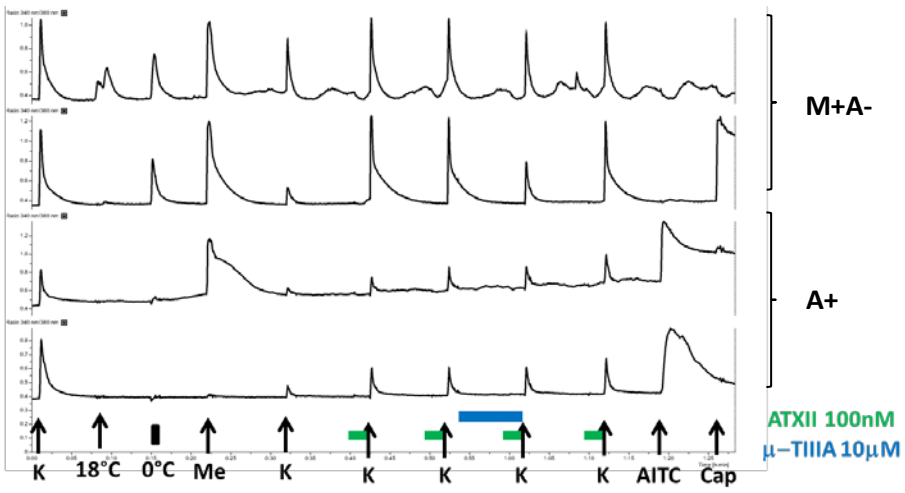

B.

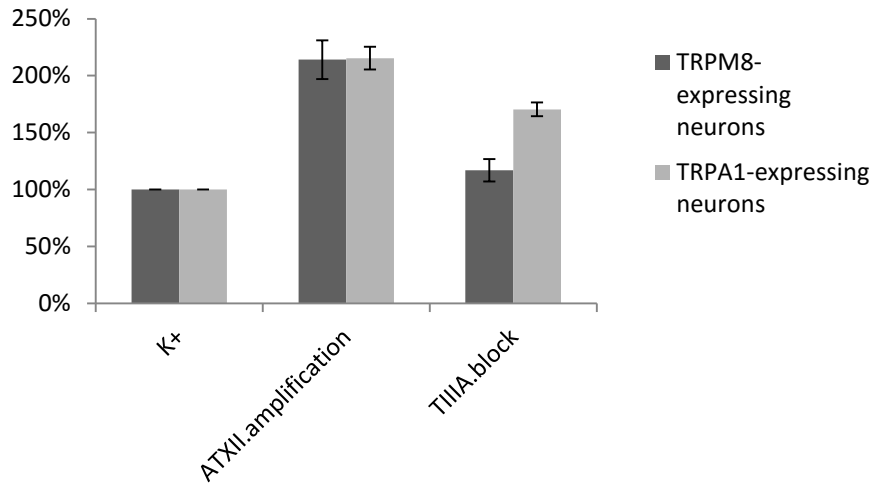

Figure 3.3: ATXII (100 nM)-elicited amplification and subsequent block by μ-TIIIA suggest expression of $Na_V1.1$ in M+A- neurons while A+ neurons (both cold-sensitive (CS) and cold-insensitive (CI)) remain mostly unaffected. Here, "K" indicates 30 mM KCl at minute 1 and then 20 mM KCl at subsequent time points. (A) Representative traces from experimental protocol where 100 nM ATXII was used to amplify K depolarization primarily mediated by $Na_V1.1$. Subsequently, conopeptide μ-TIIIA at 10 μM was used to confirm $Na_V1.1$-dependent K responses. (B) Comparison of average response peak heights of K depolarization in absence and presence of ATXII and μ-TIIIA in M+A-/TRPM8-expressing (n = 56) and A+/TRPA1-expressing neurons (n = 252).

A.

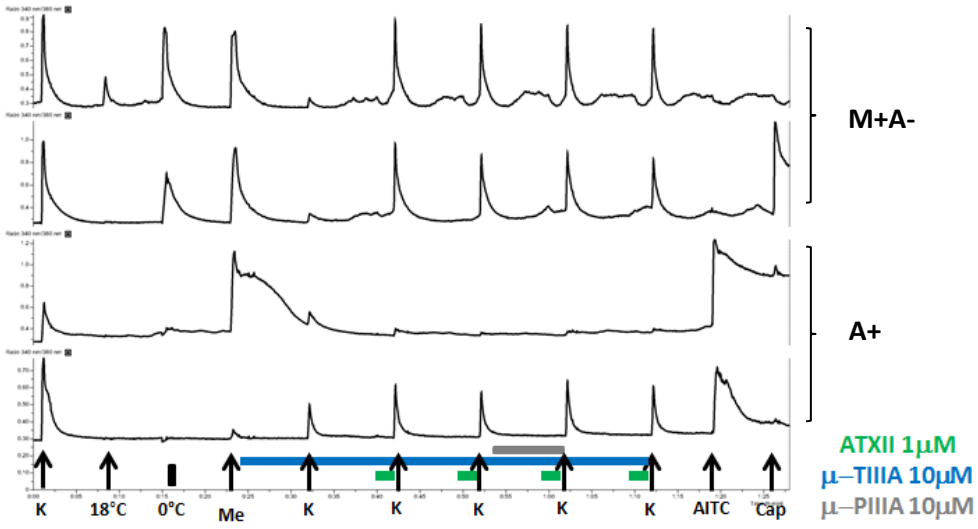

B.

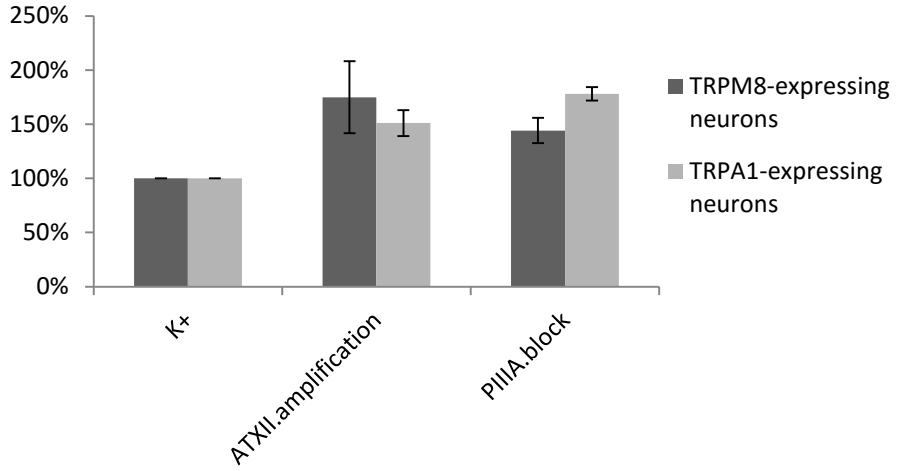

Figure 3.4: ATXII (1 μM)-elicited amplification of K depolarization was not significantly blocked by μ-PIIIA, suggesting M+A- and A+ neurons mostly do not express $Na_V1.6$. Here, "K" indicates 30 mM KCl at minute 1 and then 20 mM KCl at subsequent time points. (A) Representative traces from experimental protocol where 1 μM ATXII and 10 μM μ-TIIIA were used to amplify K depolarization primarily mediated by $Na_V1.6$. Subsequently, conopeptide μ-PIIIA at 10 μM was used to confirm $Na_V1.6$-dependent K responses. (B) Comparison of average response peak heights of K depolarization in presence of ATXII and μ-TIIIA, and μ-PIIIA in M+A-/TRPM8-expressing (n = 82) and A+/TRPA1-expressing neurons (n = 252).

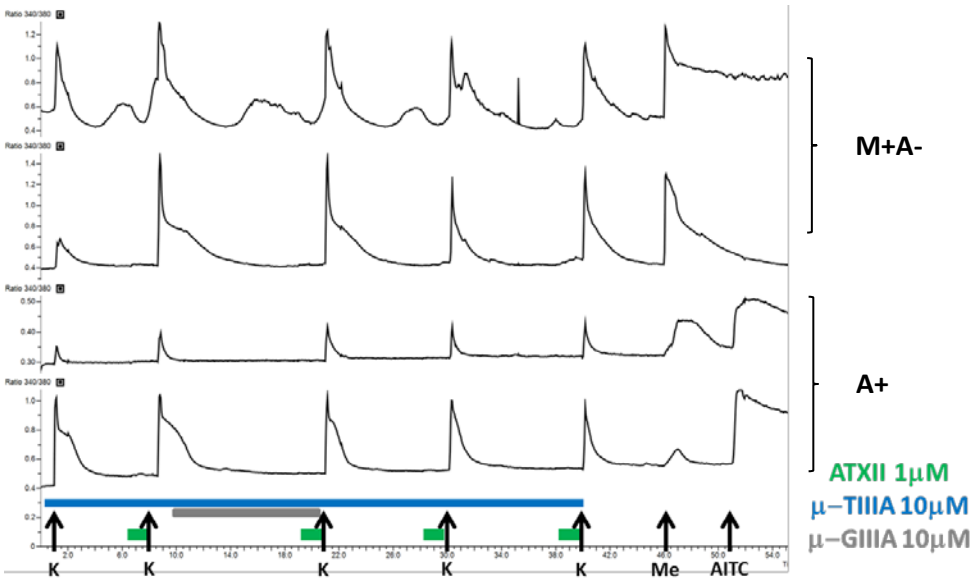

Figure 3.5: ATXII (1 μM)-elicited amplification of K depolarization was not significantly blocked by μ-GIIIA, suggesting M+A- and A+ neurons mostly do not express $Na_V1.6$. Here, "K" indicates 20 mM KCl. These are representative traces from experimental protocol where 1 μM ATXII and 10 μM μ-TIIIA were used to amplify K depolarization primarily mediated by $Na_V1.6$. Subsequently, conopeptide μ-GIIIA at 10 μM was used to confirm $Na_V1.6$-dependent K responses.

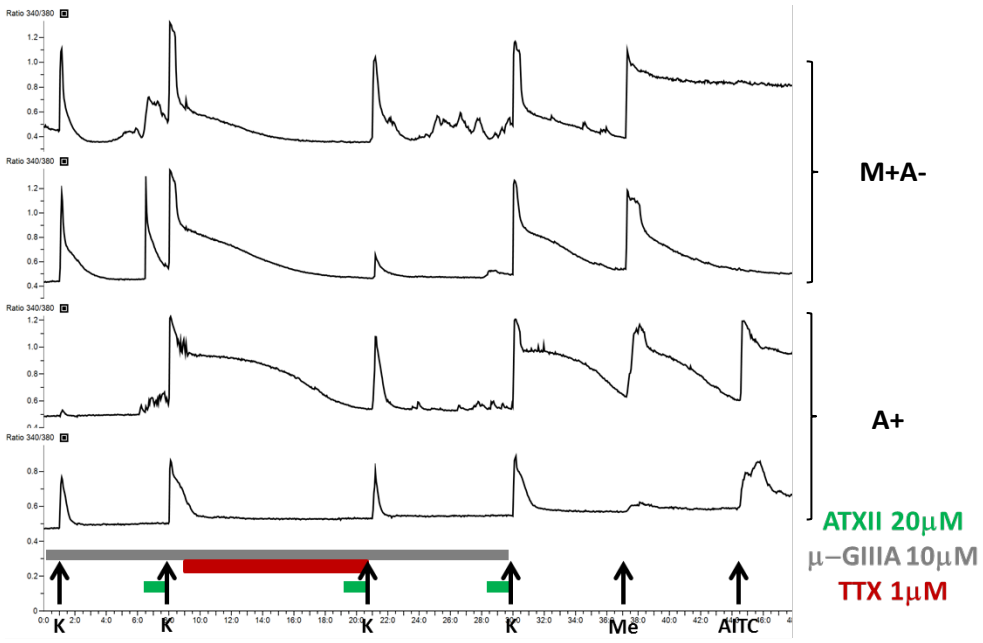

Figure 3.6: ATXII (20 μM)-elicited amplification of K depolarization and subsequent block by TTX suggest expression of $Na_V1.7$ in both M+A- neurons and A+ neurons. Here, "K" indicates 20 mM KCl. These are representative traces from experimental protocol where 20 μM ATXII and 10 μM μ-GIIIA were used to amplify K depolarization primarily mediated by $Na_V1.7$. Subsequently, TTX at 1 μM was used to confirm $Na_V1.7$-dependent K responses.

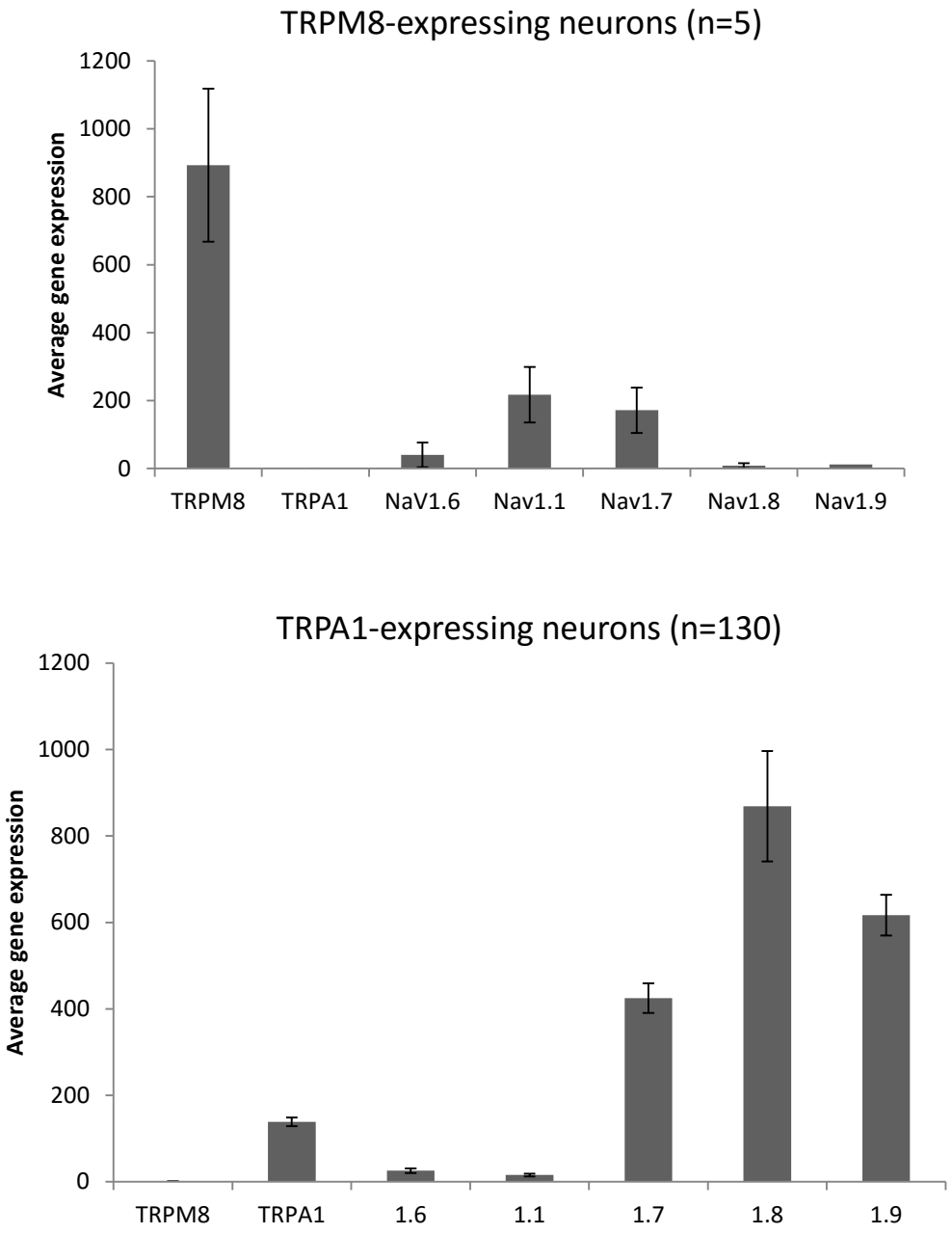

Figure 3.7: Average gene expression of Na_V channel subtypes in TRPM8- and TRPA1-expressing neurons extracted from single-cell RNA sequencing data (Usoskin et al., 2014).

CHAPTER 4

ANETHOLE OF FENNEL OIL, A SWEET AGONIST OF TRPA1 CHANNELS

Manuscript in Preparation

4.1 Background

Agonists of TRPA1 ion channel include pungent compounds and environmental irritants (Jordt et al., 2004; Bautista et al., 2005; Macpherson et al., 2007; Deering-Rice et al., 2011). Contrary to the perception of TRPA1 agonists being noxious, we find that the sweet and licorice Fennel oil can also activate TRPA1 channels in mouse sensory neurons. The sweet and licorice flavor of Fennel oil is derived from its major component *trans*-anethole, an aromatic compound also found in anise seed oil (Badgujar et al., 2014). Like Fennel oil, *trans*-anethole also activates TRPA1 channels.

The essential oil of Fennel is extracted from *Foeniculum vulgare*, a flavorful herb widely used in cooking, baking, herbal teas, and alcoholic beverages all over the world (Badgujar et al., 2014). Although chemical components of this herb are well characterized, cellular and molecular target(s) responsible for the sweet and licorice flavor remain unknown. So far, only a few studies have focused on the biological activity of fennel oil and its phenylpropene derivative *trans*-anethole (Badgujar et al., 2014). These studies have primarily evaluated antibacterial and antifungal properties of *trans*-anethole except a recent study which established its anti-inflammatory and analgesic activity in mouse models of Carrageenan and Complete Freud's adjuvant (Ritter et al., 2013). Such beneficial properties of *trans*-anethole along with the pleasant flavor possibly explain its wide use in multiple cultures and traditions for treating diseased conditions (Badgujar et al., 2014).

Here, we used calcium imaging to screen the activity of Fennel Oil (FO) and *trans*-anethole. We find that both FO and *trans*-anethole primarily activate TRPA1 channels expressed in mouse sensory neurons and HEK293 cells. Furthermore, *in vivo* activity of

trans-anethole in mice also suggests TRPA1-dependent activity. Hence, this study highlights the novel interaction of *trans*-anethole and TRPA1 channel.

4.2 Experimental Procedures

4.2.1 Cell Culture

Dorsal root ganglia (DRG), Trigeminal ganglia (TG), and HEK293 cell cultures were prepared as described previously (Chapter 2). Briefly, lumbar DRG and TG were removed, trypsinized with 0.25% trysin, and plated on polylysine-coated plates. Cultured neurons of DRG and TG were incubated with MEM overnight. Similarly, HEK 293 cells were also plated on polylysine-coated plates and incubated with DMEM:F12 media overnight for calcium imaging experiments.

4.2.2 Calcium Imaging

Neurons or HEK cells were incubated with Fura2-AM an hour before experiment. Fluorescence of Fura2, a measure of intracellular calcium, was monitored as 340 nm/ 380 nm ratio over time. DRG observation salt solution (Chapter 2) was used as bath solution and to dissolve chemicals at working concentrations. Fennel oil (Amazon) and *trans*-anethole (Sigma) solutions were made fresh before every experiment. All the chemicals including 30 mM extracellular potassium $[K^+]_O$ were applied to neurons or cells for 15 seconds.

4.2.3 GC-MS

GC-MS analysis of Fennel oil and *trans*-anethole was carried out by Alan Maschek (HSC Cores-Metabolomics, University of Utah). Samples (1 µL) were resuspended into 1 mL of EtOAc and transferred into a glass GC/MS vial for analysis. GC/MS analyses were conducted using an HP6890 instrument interfaced with an MSD-HP5973 detector and equipped with a Zebron ZB-5MSi Guardian (30 m x 0.25 mm ID, 0.25 µm film thickness; Phenomenex) column and an HP7682 injector. Helium was used as a carrier gas at a flow rate of 13.8 mL/min with a 10:1 split ratio at an injection volume of 1 µL. The injector temperature was 250 °C. The oven temperature gradient was programmed as follows: 50 °C held for 1 minute increased at a rate of 40 °C/min to 65 °C, held for 1 minute, increased at a rate of 40 °C/min to 330 °C and held for 5 minutes. MS spectra were obtained in EI mode from a range of m/z 40 – 400. The MS quad temperature was 150 °C, MS source temperature is 230 °C, solvent cut time of 2.5 minutes, and scanned at 4 scans/sec. Data was first collected on an Agilent MSD Chemstation, translated using an Agilent GC MSD translator, then analyzed using Agilent MassHunter Quant and the NIST14 library.

4.2.4 Behavioral Assays

Two types of behavioral assays were used to evaluate the *in vivo* activity of *trans*-anethole in mice. First, subcutaneous injection of 20 µL of either *trans*-anethole or AITC or vehicle (DRG obs.) were injected in left hindpaw of mice both males and females. The nocifensive behavior such as paw lifting and licking behavior following injection were then observed for 30 minutes.

As TRP channels contribute to the sense of chemical and noxious stimuli (Roper, 2014), we adapted the drinking preference assay from previous studies (Kwan et al., 2006; Everaerts et al., 2011). Mice were deprived of water for a day and red cap (of 50 mL tubes) containing either water or *trans*-anethole or AITC and another red cap containing only water were placed in two opposite corners of the cage. The drinking preference of these mice to the chemicals was then observed for 5 minutes and compared to that of water only condition.

4.2.5 Data Analysis

Calcium imaging data was subjected to binary scoring as described in Chapter 2. A response to a given stimulus was considered positive, if the 340nm/ 380nm ratio change was > 0.05 from baseline. Percentage of responsive neurons ($[K^+]_O$ responsive) or cells, averaged across multiple experiments and cultures, is presented as response frequency ± SEM for a given stimulus. Total number of neurons or cells scored for each experimental condition is indicated in respective figure legends.

Nocifensive responses such as paw licking and lifting to subcutaneous injections in mice were scored by observing each mouse for 30 minutes post injection. During this time period, the duration (seconds) of paw licking and lifting behavior was recorded and averaged for a given treatment. One-way ANOVA and post-hoc t test were used to test the differences between experimental groups. Experiments with drinking preference assay are underway and will be quantified in future.

4.3 Results

As a variety of odorants and tastants like menthol, mustard oil or AITC, and capsaicin target TRP channels (Caterina et al., 1997; Jordt et al., 2004; Bautista et al., 2007; Roper, 2014; Friedland and Harteneck, 2017), we used these TRP channel agonists to identify neuronal cell-types stimulated by FO and anethole (for *trans*-anethole). We also screened the activity of FO and anethole on human TRPA1 channel expressed in HEK293 cells. Lastly, multiple behavioral assays were used to assess *in vivo* effects of licorice anethole.

4.3.1 FO Activates Mouse and Human TRPA1 Channels

Using calcium imaging, we tested different dilutions of fennel oil (FO). As 10,000-fold dilution of FO showed robust responses in a subset of mouse sensory neurons, we used this dilution to determine the specific neuronal cell-type activated by FO. We employed TRP channel agonists such as, menthol, AITC (MO), and capsaicin to identify these neuronal cell-types expressing TRPM8, TRPA1, and TRPV1, respectively (Chapter 2) (Teichert et al., 2012a, 2012b, 2014). To our surprise, the sweet and licorice FO (1:10,000) selectively activated a subset of AITC-sensitive (TRPA1-expressing) neurons (Figure 4.1A, 4.1B, & 4.1C). On average, ~90% of FO-sensitive neurons were AITC-sensitive (Figure 4.1B). These FO elicited responses were blocked by 30 μM HC-030031, a selective TRPA1 antagonist (Eid et al., 2008), suggesting direct activation of mouse TRPA1 by FO component(s) (Figure 4.1D). To further confirm the activity of FO on TRPA1, we tested dilutions of FO on HEK293 cells overexpressing human TRPA1 channels. Again, FO activated the human TRPA1 channel in a dose-dependent manner without eliciting any response in untransfected HEK293 cells (Figure 4.1E & 4.1F).

Cumulatively, these results with mouse sensory neurons and HEK293 cells strongly suggested that a component of FO activates both mouse and human TRPA1 channels.

4.3.2 *trans*-anethole Is the Major Component of FO

As FO is extracted from the herb *Foeniculum vulgare*, it may contain a complex mixture of chemical components. To determine a specific chemical component responsible for the activation of TRPA1 channels, we subjected FO to GC-MS analysis. Indeed, FO had multiple components with *trans*-anethole being the most abundant (Table 4.1). The presence of anethole was confirmed using the NIST14 library and *trans*-anethole as a standard (Figure 4.2). As shown in Table 4.1, *trans*-anethole makes up about ~75% of FO. Therefore, we hypothesized that *trans*-anethole may mimic the activity of FO on TRPA1.

4.3.3 *trans*-anethole Mimics FO Activity on TRPA1 Channels

Different concentrations of *trans*-anethole were tested on sensory neurons of mouse DRG. Like FO, 130 μM of anethole robustly activated a subset of TRPA1 expressing (AITC-sensitive) neurons (Figure 4.3A, 4.3B & 4.3C). On average, ~94% of anethole responding neurons were AITC-sensitive (Figure 4.3B). These anethole-elicited responses in mouse sensory neurons were also completely blocked by TRPA1 blocker, HC-030031, suggesting direct activation of mouse TRPA1 channels (Figure 4.3D). Anethole also activated human TRPA1 channels expressed in HEK293 cells in a dose-dependent manner without eliciting any response in untransfected HEK cells (Figure 4.3E & 4.3F). Hence, these results with *trans*-anethole cumulatively suggest that the activity of

FO on TRPA1 channels is mainly due to its major component, *trans*-anethole.

As TRP channel agonists mediate chemesthesis via sensory neurons of trigeminal ganglia, we also tested activity of anethole on these neurons. Again, 130 μM anethole selectively activates AITC-sensitive TG neurons (Figure 4.4). Thus, TRPA1-expressing TG neurons involved in chemesthesis most likely mediate the chemical sense of licorice anethole along with that of pungent AITC.

4.3.4 *trans*-anethole Induces Mild Nocifensive Responses in Mice

TRP channel agonists are not only perceived as pungent and noxious but can also elicit nocifensive behaviors such as paw lifting and licking in mice when injected subcutaneously. Therefore, we tested if the sweet and licorice anethole also elicits nocifensive responses in mice. Despite the pleasant perception of anethole, subcutaneous injection of 20 μL anethole in mouse hindpaw did induce mild paw licking behavior in mice (Figure 4.5). However, even high concentrations of anethole induced only mild responses when compared to one induced by 10 mM AITC. Also, anethole treatment did not induce a paw lifting response like AITC did (data not shown). Nonetheless, these experiments suggested that anethole does not only activate TRPA1 *in vitro* but also *in vivo*.

Mice when given drinking water containing AITC show aversion, which has been attributed to TRPA1 activation in TG sensory neurons (Kwan and Corey, 2009; Everaerts et al., 2011). As anethole also activates TRPA1-expressing TG neurons, mice were given drinking water with and without anethole or AITC, and their drinking preference was assessed (Figure 4.6). Mice did show aversion to anethole but preliminary observations

suggest this aversion to anethole is mild when compared to AITC. Hence, we will continue to test and quantify the drinking preference of mice at different concentrations of anethole in both WT and TRPA1-/- mice.

4.4 Discussion

In this study, we have identified TRPA1 channel as the primary molecular target of FO and its active compound *trans*-anethole in somatosensory neurons. However, anethole activated only a subset of AITC responsive DRG (56%) and TG (79%) neurons and anethole-induced calcium increase was also weak and transient compared to AITC (Figure 4.3C). Nocifensive behaviors such as paw licking and aversion to drinking water induced by anethole were also mild compared to AITC. Thus, both *in vitro* and *in vivo* assays suggest that anethole is probably a weaker agonist of the TRPA1 channel in comparison to AITC.

TRPA1, like TRPV1, is considered a nociceptive ion channel (McNamara et al., 2007; Kremeyer et al., 2010; Bautista et al., 2013). Therefore, antagonists of TRPA1 channel have been developed for pain relief (Eid et al., 2008; Zhao et al., 2012; Gui et al., 2014). However, treatment with anethole, a TRPA1 agonist, can also be analgesic and anti-inflammatory in mouse models of pain (Ritter et al., 2013). Similar observations have been made with other TRPA1 agonists (Leamy et al., 2011; Chung et al., 2013; Zhai et al., 2014; Bressan et al., 2016; Kaimoto et al., 2016). These TRPA1 agonists assert analgesic activity by activating and subsequently desensitizing TRPA1 channels (Story et al., 2003; Akopian et al., 2007; Leamy et al., 2011; Zhai et al., 2014; Bressan et al., 2016; Kaimoto et al., 2016). To test if analgesic activity of anethole results from TRPA1

desensitization, we gave repetitive application of anethole to HEK293 cells expressing human TRPA1 channel. As shown in Figure 4.7, anethole-induced calcium increase does desensitize with repetitive applications. Thus, it is possible that anehole, like other TRPA1 (and also TRPV1) agonists, induces acute pain but long-term pain relief by desensitizing TRPA1 channel.

Even though we identified TRPA1 as the primary molecular target of anethole in somatosensory neurons, it still remains unclear why two agonists of the same ion channel result in different perceptions. Besides somatosensation, gustation and olfaction also contribute to the perception of flavors. The sense of odor is detected by GPCRs in olfactory sensory neurons (OSNs) innervating olfactory epithelium of nose whereas the sense of taste is detected by GPCRs in taste receptor cells (TRCs) of tongue (Furudono et al., 2009; Chaudhari and Roper, 2010; Roper, 2014; Friedland and Harteneck, 2017). Although TRP channels are found in olfactory epithelium and tongue, their direct involvement in detecting various odorants and tastants remains debatable (Xu et al., 2006; Venkatachalam and Montell, 2007; Damann et al., 2008; Spehr and Munger, 2009; Economo et al., 2016; Friedland and Harteneck, 2017). Hence, to understand our sense of the sweet, licorice, and pungent flavors, contribution of TRPA1 channels to olfaction and gustation must be evaluated.

4.5 References

Akopian AN, Ruparel NB, Jeske NA, Hargreaves KM (2007) Transient receptor potential TRPA1 channel desensitization in sensory neurons is agonist dependent and regulated by TRPV1-directed internalization. J Physiol 1:175–193.

Badgujar SB, Patel VV, Bandivdekar AH (2014) Foeniculum vulgare mill: a review of its botany, phytochemistry, pharmacology, contemporary application, and toxicology. Biomed Res Int 2014:842674.

Bautista DM, Movahed P, Hinman A, Axelsson HE, Sterner O, Högestätt ED, Julius D, Jordt S-E, Zygmunt PM (2005) Pungent products from garlic activate the sensory ion channel TRPA1. Proc Natl Acad Sci U S A 102:12248–12252 Available at: http://www.pubmedcentral.nih.gov/articlerender.fcgi?artid=1189336&tool=pmcentrez&rendertype=abstract.

Bautista DM, Pellegrino M, Tsunozaki M (2013) TRPA1: a gatekeeper for inflammation. Annu Rev Physiol 75:181–200.

Bautista DM, Siemens J, Glazer JM, Tsuruda PR, Basbaum AI, Stucky CL, Jordt S-E, Julius D (2007) The menthol receptor TRPM8 is the principal detector of environmental cold. Nature 448:204–208.

Bressan E, Touska F, Vetter I, Kistner K, Kichko TI, Teixeira B, Picolo G, Cury Y, Lewis RJ, Fischer MJM (2016) Crotalphine desensitizes TRPA1 ion channels to alleviate inflammatory hyperalgesia. PAIN 157:2504–2516.

Caterina MJ, Schumacher MA, Tominaga M, Rosen TA, Levine JD, Julius D (1997) The capsaicin receptor: a heat-activated ion channel in the pain pathway. Nature 389:816–824 Available at: http://www.ncbi.nlm.nih.gov/pubmed/9349813.

Chaudhari N, Roper SD (2010) The cell biology of taste. JCB 190:285–296.

Chung G, Im S, Kim YH, Jung SJ, Rhyu M-R, Oh SB (2013) Activation of transient receptor potential ankyrin 1 by eugenol. Neuroscience 261:153-60 Available at: http://linkinghub.elsevier.com/retrieve/pii/S0306452213010725 [Accessed January 4, 2014].

Damann N, Voets T, Nilius B (2008) TRPs in our senses. Current Biology 18:880–889.

Deering-Rice CE, Romero EG, Shapiro D, Hughen RW, Light AR, Yost GS, Veranth JM, Reilly C a (2011) Electrophilic components of diesel exhaust particles (DEP) activate transient receptor potential ankyrin-1 (TRPA1): a probable mechanism of acute pulmonary toxicity for DEP. Chem Res Toxicol 24:950–959 Available at: http://www.pubmedcentral.nih.gov/articlerender.fcgi?artid=3133601&tool=pmcentrez&rendertype=abstract.

Economo MN, Hansen KR, Economo MN, Hansen KR, Wachowiak M (2016) Control of mitral / tufted cell output by selective inhibition among olfactory bulb glomeruli article control of mitral / tufted cell output by selective inhibition among olfactory bulb glomeruli. Neuron 91:397–411.

Eid SR, Crown ED, Moore EL, Liang HA, Choong K-C, Dima S, Henze DA, Kane SA, Urban MO (2008) HC-030031, a TRPA1 selective antagonist, attenuates inflammatory- and neuropathy-induced mechanical hypersensitivity. Mol Pain 4:48.

Everaerts W, Gees M, Alpizar YA, Farre R, Leten C, Apetrei A, Dewachter I, Van Leuven F, Vennekens R, De Ridder D, Nilius B, Voets T, Talavera K (2011) The

capsaicin receptor TRPV1 is a crucial mediator of the noxious effects of mustard oil. Curr Biol 21:316–321.

Friedland K, Harteneck C (2017) Spices and odorants as TRP channel activators. In: Springer Handbook of Odor (Buettner A, ed), pp 85–86. Cham: Springer International Publishing. Available at: http://dx.doi.org/10.1007/978-3-319-26932-0_34.

Furudono Y, Sone Y, Takizawa K, Hirono J, Sato T (2009) Relationship between peripheral receptor code and perceived odor quality. Chem Senses 34:151–158.

Gui J, Liu B, Cao G, Lipchik AM, Perez M, Dekan Z, Mobli M, Daly NL, Alewood PF, Parker LL, King GF, Zhou Y, Jordt SE, Nitabach MN (2014) A tarantula-venom peptide antagonizes the TRPA1 nociceptor Ion channel by binding to the S1-S4 gating domain. Curr Biol 24(5):473-483.

Jordt S-E, Bautista DM, Chuang H-H, McKemy DD, Zygmunt PM, Högestätt ED, Meng ID, Julius D (2004) Mustard oils and cannabinoids excite sensory nerve fibres through the TRP channel ANKTM1. Nature 427:260–265.

Kaimoto T, Hatakeyama Y, Takahashi K, Imagawa T, Tominaga M, Ohta T (2016) Involvement of transient receptor potential A1 channel in algesic and analgesic actions of the organic compound limonene. Eur J Pain 20(7):1155–1165.

Kremeyer B et al. (2010) A gain-of-function mutation in trpa1 causes familial episodic pain syndrome. Neuron 66:671–680.

Kwan KY, Allchorne AJ, Vollrath MA, Christensen AP, Zhang DS, Woolf CJ, Corey DP (2006) TRPA1 contributes to cold, mechanical, and chemical nociception but is not essential for hair-cell transduction. Neuron 50:277–289.

Kwan KY, Corey DP (2009) Burning cold: involvement of TRPA1 in noxious cold sensation. J Gen Physiol 133:251–256.

Leamy AW, Shukla P, McAlexander M a., Carr MJ, Ghatta S (2011) Curcumin ((E,E)-1,7-bis(4-hydroxy-3-methoxyphenyl)-1,6-heptadiene-3,5-dione) activates and desensitizes the nociceptor ion channel TRPA1. Neurosci Lett 503:157–162 Available at: http://dx.doi.org/10.1016/j.neulet.2011.07.054.

Macpherson LJ, Dubin AE, Evans MJ, Marr F, Schultz PG, Cravatt BF, Patapoutian A (2007) Noxious compounds activate TRPA1 ion channels through covalent modification of cysteines. Nature 445:541–545.

McNamara CR, Mandel-Brehm J, Bautista DM, Siemens J, Deranian KL, Zhao M, Hayward NJ, Chong J a, Julius D, Moran MM, Fanger CM (2007) TRPA1 mediates formalin-induced pain. Proc Natl Acad Sci U S A 104:13525–13530 Available at: http://www.pubmedcentral.nih.gov/articlerender.fcgi?artid=1941642&tool=pmcentrez&rendertype=abstract.

Ritter AM V, Domiciano TP, Verri Jr. WA, Zarpelon AC, da Silva L, Barbosa CP, Natali MRM, Cuman RKN, Bersani-Amando CA (2013) Antihypernociceptive activity of anethole in experimental inflammatory pain. Inflammopharmacol 21(2):187-97.

Roper SD (2014) TRPs in taste and chemesthesis. In: Mammalian Transient Receptor Potential (TRP) Cation Channels: Volume II (Nilius B, Flockerzi V, eds), pp 827–871.

Spehr M, Munger SD (2009) Olfactory receptors: G protein-coupled receptors and beyond. J Neurochem 109:1570–1583.

Story GM, Peier AM, Reeve AJ, Eid SR, Mosbacher J, Hricik TR, Earley TJ, Hergarden AC, Andersson D a, Hwang SW, McIntyre P, Jegla T, Bevan S, Patapoutian A (2003) ANKTM1, a TRP-like channel expressed in nociceptive neurons, is activated by cold temperatures. Cell 112:819–829.

Teichert RW, Memon T, Aman JW, Olivera BM (2014) Using constellation pharmacology to define comprehensively a somatosensory neuronal subclass. Proc Natl Acad Sci U S A 111:2319–2324.

Teichert RW, Raghuraman S, Memon T, Cox JL, Foulkes T, Rivier JE, Olivera BM (2012a) Characterization of two neuronal subclasses through constellation pharmacology. Proc Natl Acad Sci U S A 109(31):12758–63.

Teichert RW, Smith NJ, Raghuraman S, Yoshikami D, Light AR, Olivera BM (2012b) Functional profiling of neurons through cellular neuropharmacology. Proc Natl Acad Sci U S A 109:1388–1395.

Venkatachalam K, Montell C (2007) TRP channels. Annu Rev Biochem 76:387–417 Available at: http://www.ncbi.nlm.nih.gov/pubmed/17579562 [Accessed September 23, 2013].

Xu H, Delling M, Jun JC, Clapham DE (2006) Oregano, thyme and clove-derived flavors and skin sensitizers activate specific TRP channels. Nat Neurosci 9(5):628–35.

Zhai C, Liu Q, Zhang Y, Wang S, Zhang Y, Li S, Qiao Y (2014) Identification of natural compound carnosol as a novel TRPA1 receptor agonist. Molecules 19:18733–18746 Available at: http://www.mdpi.com/1420-3049/19/11/18733/htm.

Zhao M, Isami K, Nakamura S, Shirakawa H, Nakagawa T, Kaneko S (2012) Acute cold hypersensitivity characteristically induced by oxaliplatin is caused by the enhanced responsiveness of TRPA1 in mice. Mol Pain 8:55 Available at: http://www.pubmedcentral.nih.gov/articlerender.fcgi?artid=3495669&tool=pmcentrez&rendertype=abstract.

Table 4.1: GC-MS analysis of fennel oil

Constituents	Retention time	Percentage (%)
alpha-Phellandrene	2.681-2.702	2.7
D-Limonene	2.883-2.921	2.9
Fenchone	3.310-3.326	15.03
Estragole	3.896-3.913	3.9
trans-Anethole	4.28-4.306	78.22

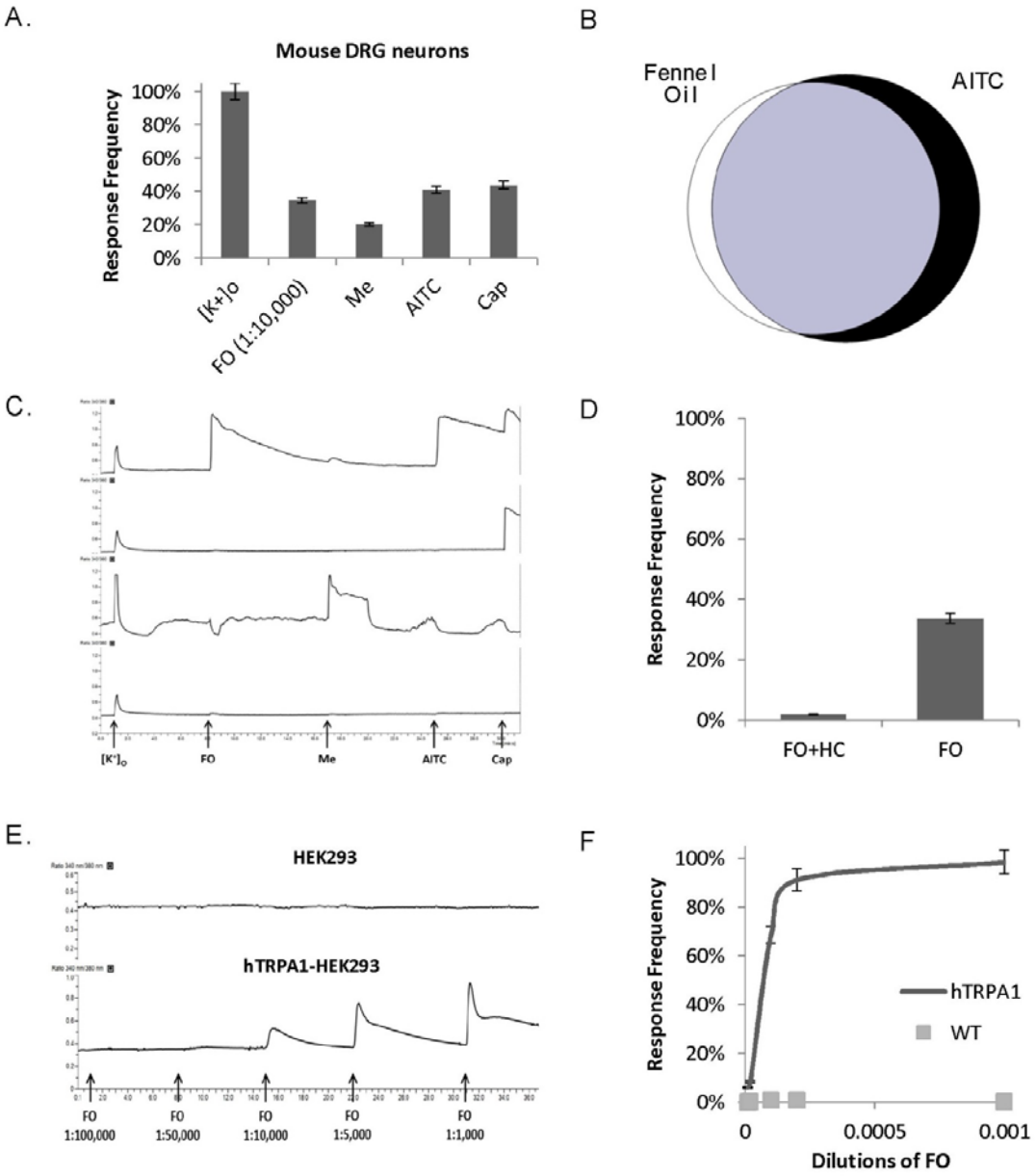

Figure 4.1: FO activates mouse and human TRPA1 channels. (A) Response frequency of mouse DRG neurons (n = 1328) to given stimuli. (B) Overlap between FO and AITC responsive neurons. (C) Representative calcium imaging traces of neuronal phenotypes observed. (D) Response frequency of FO (1:10,000) in presence and absence of 30 μM HC-030031, a selective TRPA1 antagonist. (E) Dose-response of FO in untransfected and human TRPA1-expressing HEK293 cells. (F) Response frequency of HEK cells to various dilutions of FO.

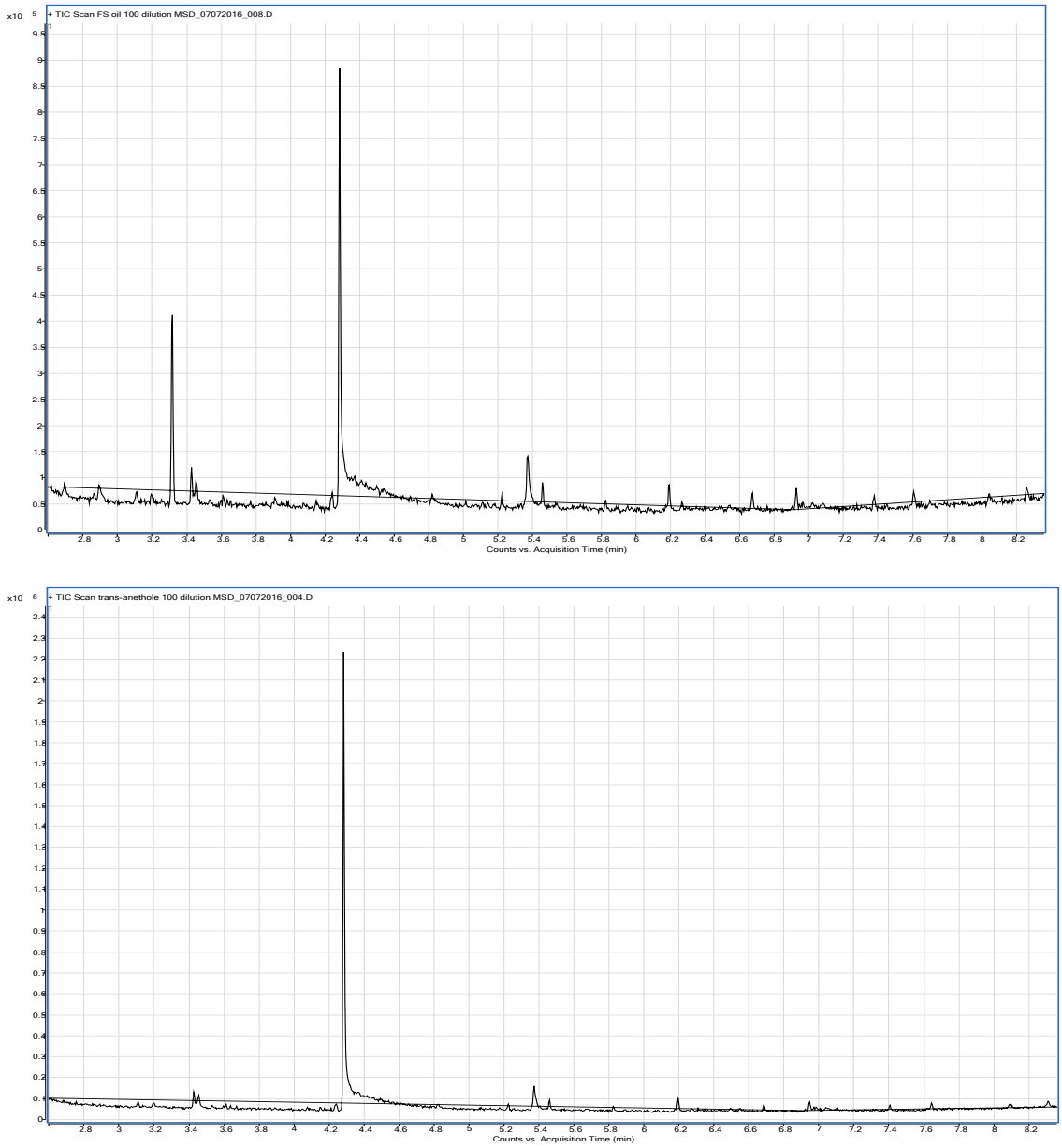

Figure 4.2: GC-MS profile of FO (top) and *trans*-anethole (bottom)

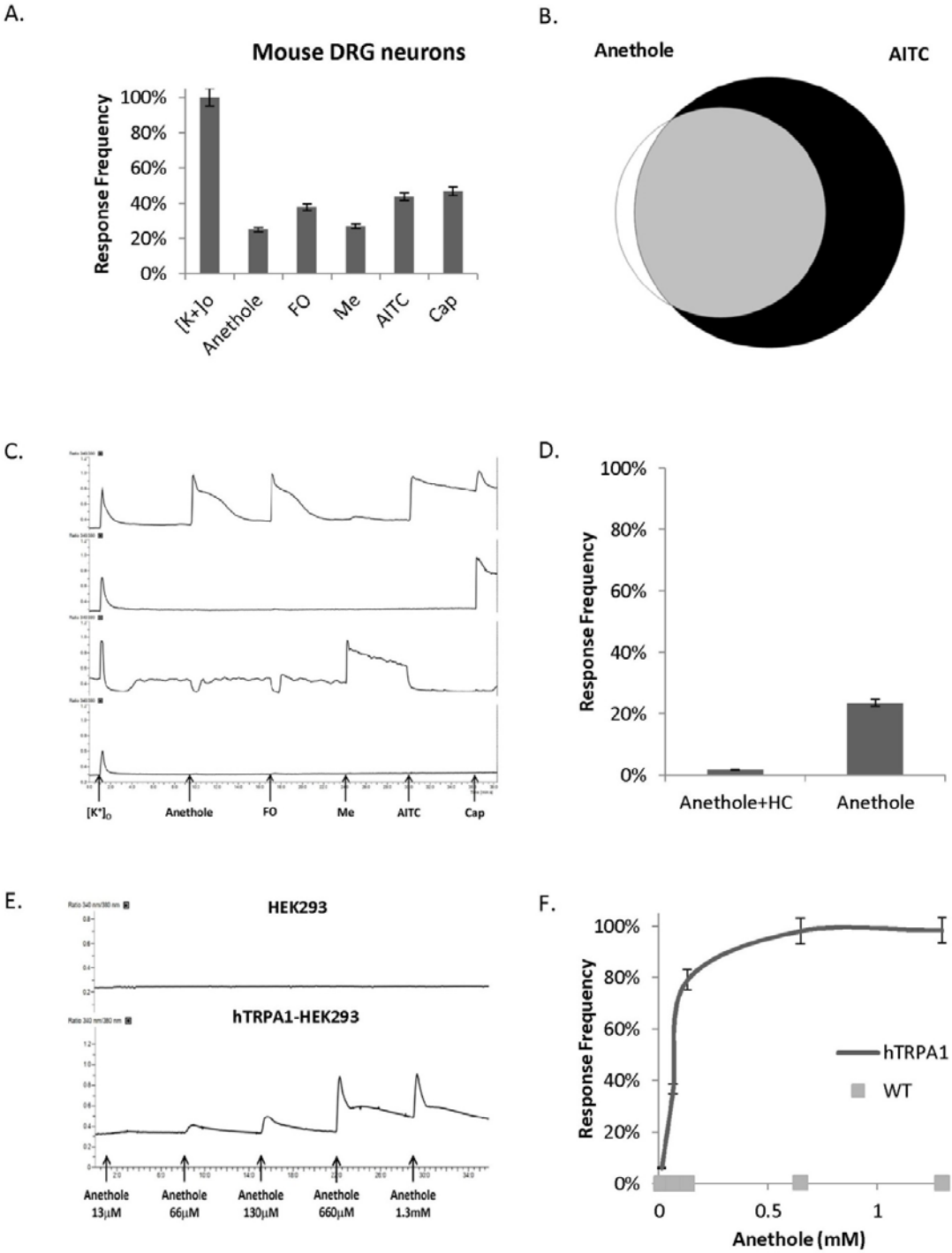

Figure 4.3: *trans*-anethole mimics activity of FO on TRPA1 channels. (A) Response frequency of mouse DRG neurons (n = 1375) to respective stimuli. (B) Overlap between *trans*-anethole and AITC responsive neurons. (C) Representative calcium imaging traces of neuronal phenotypes observed. (D) Response frequency of anethole (130 μM) in presence and absence of 30 μM HC-030031, a selective TRPA1 antagonist. (E) Dose-response of anethole in untransfected and human TRPA1-expressing HEK293 cells. (F) Response frequency of HEK cells to various concentrations of anethole.

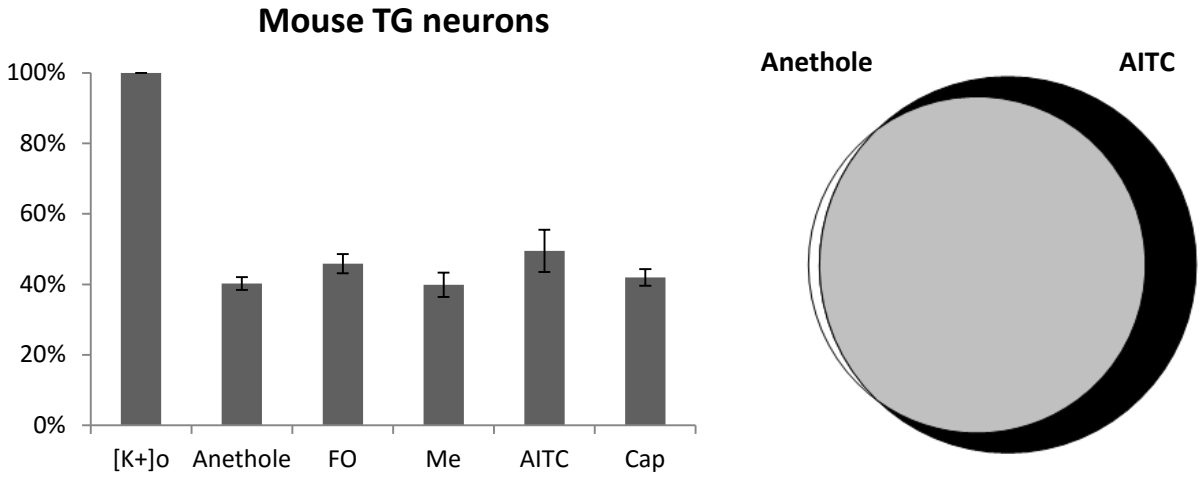

Figure 4.4: *trans*-anethole mimics activity of FO on TRPA1 channels in TG neurons. (A) Response frequency of mouse TG neurons (n = 964) to given stimuli. (B) Overlap between *trans*-anethole and AITC responsive TG neurons.

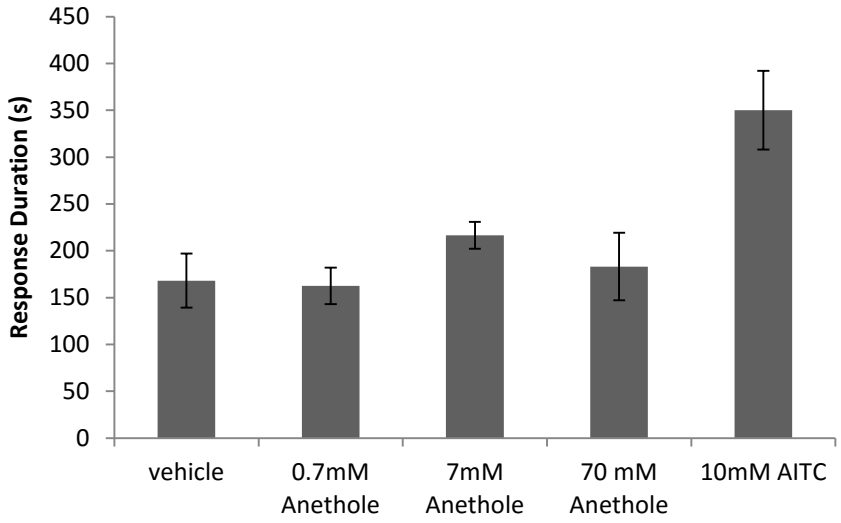

Figure 4.5: Subcutaneous injection of *trans*-anethole induces mild nocifensive behavior in mice. Response duration (seconds) ± SEM of paw licking was monitored over 30 minutes post injection of vehicle (n =3), and 0.7 mM (n=3), 7 mM (n=3), and 70 mM (n=2) anethole, and 10 mM AITC (n=3).

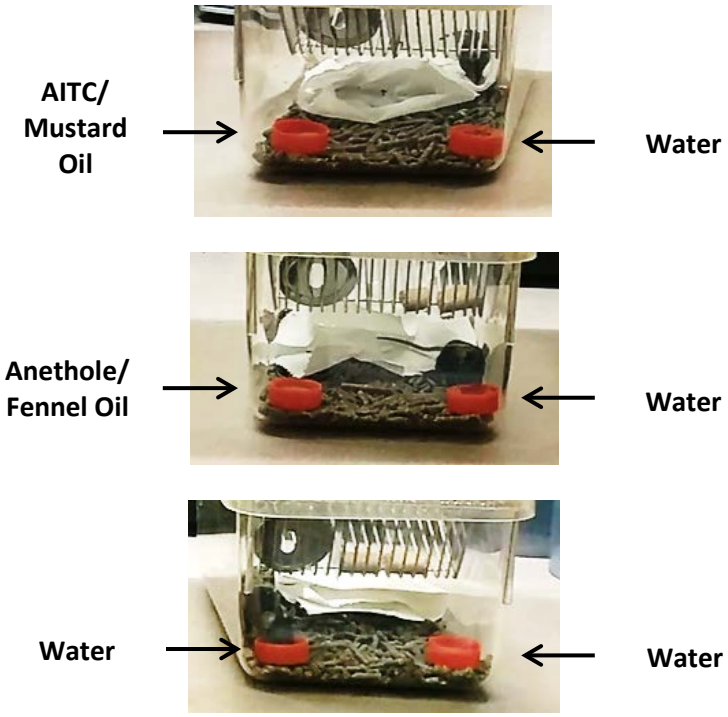

Figure 4.6: An assay developed to asses drinking preference of mice to anethole and AITC.

A.

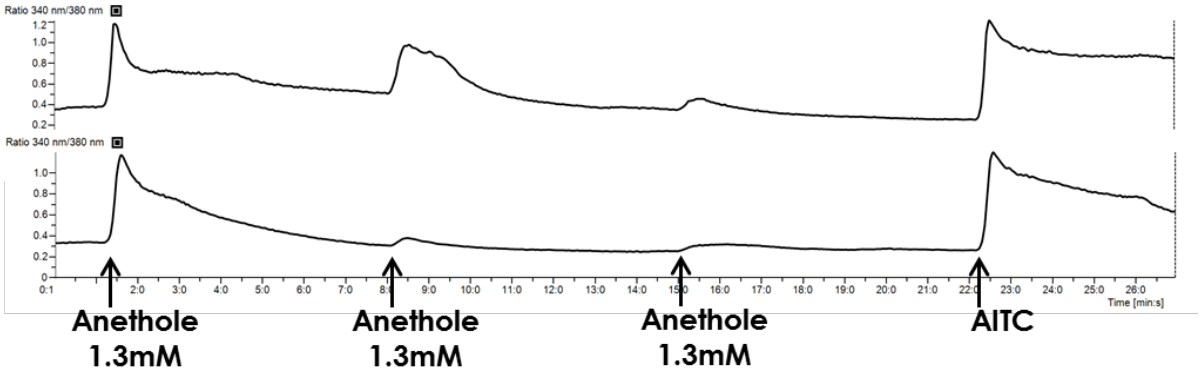

B.

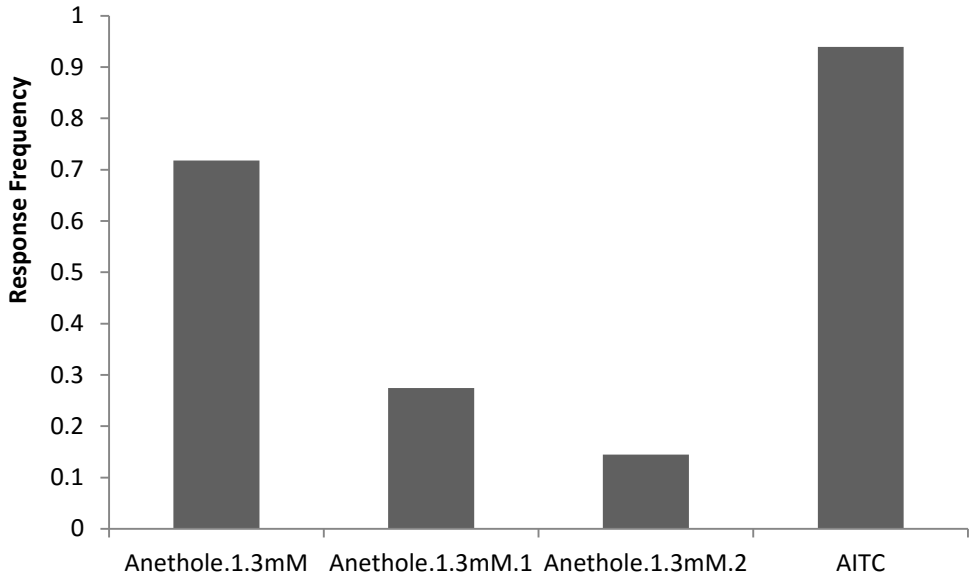

Figure 4.7: Desensitization of anethole-induced calcium responses in hTRPA1-HEK293 cells. (A) Representative traces illustrating desensitization of anethole responses. (B) Response frequency of hTRPA1-HEK293 cells to repetitive application of 1.3 mM anethole and 100 μMAITC.

CHAPTER 5

CONCLUSION

Constellation of ion channels (K_V and Na_V) expressed in TRPM8- versus TRPA1-expressing neurons suggests that TRPM8-expressing neurons are responsible for innocuous cold-sensation whereas cold-sensitive TRPA1-expressing neurons are responsible for noxious cold-sensation (Figure 5.1). In addition to K_V and Na_V channels, we have also studied functional expression of TRPV1 channel, voltage-gated calcium (Ca_V) channels, ATP receptors, and nicotinic acetylcholine receptors (nAChRs) in these neuronal cell-types (summarized in Table 5.1) (Teichert et al., 2012, 2014; Smith et al., 2013). Consistent with the role of a nociceptor, TRPA1-expressing neurons from adult mouse express ATP receptors whereas TRPM8 expressing neurons do not (Teichert et al., 2012). TRPV1 is also highly coexpressed with TRPA1 and not as much with TRPM8, further endorsing the role of TRPA1 in nociception.

The role of TRPA1-expressing neurons as nociceptors is counterintuitive to our results with sweet and licorice fennel oil and *trans*-anethole selectively targeting TRPA1-expressing neurons. However, behavioral assays in mice also hint at TRPA1-dependent activity of *trans*-anethole. In collaboration with Charles Zucker's lab, we are currently evaluating activity of *trans*-anethole on taste buds and in turn learn about the role of TRPA1 in gustation. Furthermore, contribution of TRPA1 to olfaction must also be determined in order to understand the difference in perception caused by pungent AITC and licorice *trans*-anethole. Hence, using constellation pharmacology, we could not only identify functional differences between cold-sensitive neurons but also discover the previously unknown role of TRPA1 in sensing sweet and licorice chemical.

5.1 References

Smith NJ, Hone AJ, Memon T, Bossi S, Smith TE, Mcintosh JM, Olivera BM, Teichert RW (2013) Comparative functional expression of nAChR subtypes in rodent DRG neurons. Front Cell Neurosci 7:1–11.

Teichert RW, Memon T, Aman JW, Olivera BM (2014) Using constellation pharmacology to define comprehensively a somatosensory neuronal subclass. Proc Natl Acad Sci U S A 111:2319–2324.

Teichert RW, Raghuraman S, Memon T, Cox JL, Foulkes T, Rivier JE, Olivera BM (2012) Characterization of two neuronal subclasses through constellation pharmacology. Proc Natl Acad Sci U S A 109:1–6.

Table 5. 1: Constellation pharmacology of TRPM8- and TRPA1-expressing DRG neurons from adult mouse.

Proteins	**Low-Threshold Cold Thermosensor (LT M+A-)**	**High-Threshold Cold Thermosensor (HT M+A-)**	**Cold Nociceptor (CS A+)**	**Nociceptor (CI A+)**
TRPM8	Yes	Yes	No	No
TRPA1	No	No	Yes	Yes
K_V channels	Low K_V1.1/1.2	High K_V1.1/1.2	K_V1.1/1.2	K_V1.1/1.2
Na_V channels	Na_V 1.1, 1.7	Na_V 1.1, 1.7	Na_V 1.7, 1.8 & 1.9	Na_V 1.7, 1.8 & 1.9
Ca_V channels	Predominantly Ca_V1	Predominantly Ca_V1	Mix of Ca_V1 and Ca_V2	Mix of Ca_V1 and Ca_V2
TRPV1	Low	Low	High	High
ATP receptors	No	No	Yes	Yes
nAChRs	α7	α7	Mix of α7 & α3β4 / α6β4	Mix of α7 & α3β4 / α6β4

Adapted from Teichert et al., 2012.

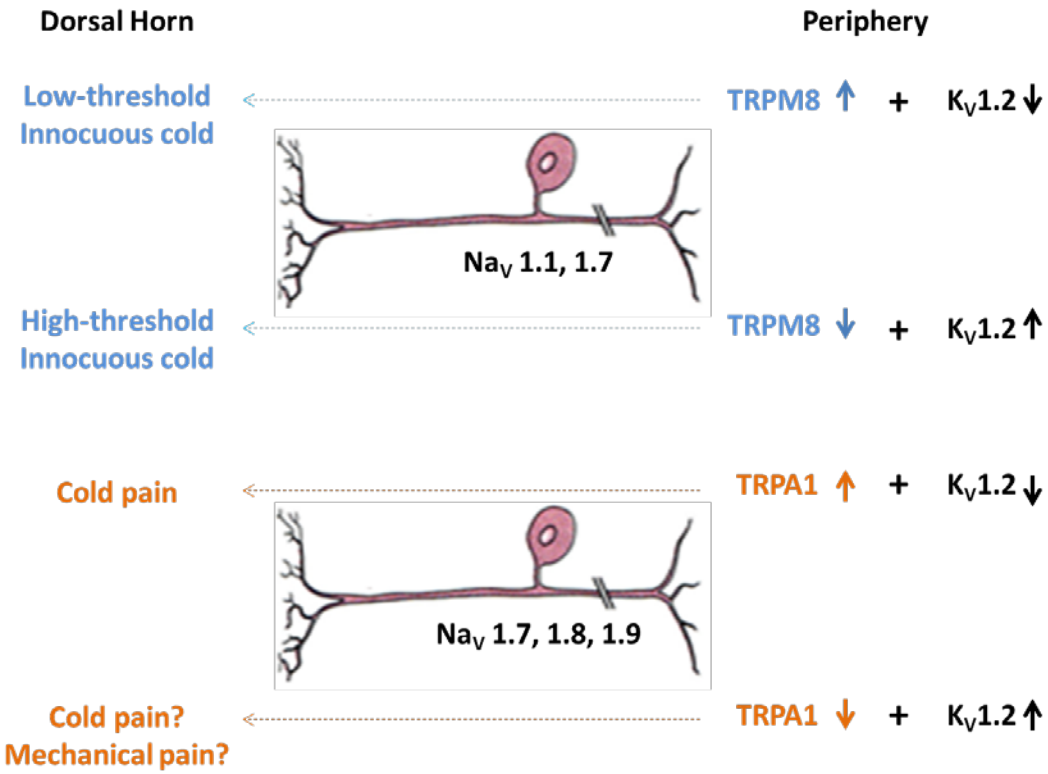

Figure 5.1: Proposed model for role of TPRM8- and TRPA1-expressing neurons in cold-sensation. TRPM8-expressing neurons detect either low or high threshold innocuous cold temperature in periphery depending on expression of TRPM8 and K_V1.2 (and other K_V channel too) channels. The sensation of innocuous cold-sensation is then propagated to the dorsal horn of spinal cord by Na_V1.1 and 1.7. Under extreme cold conditions, cold-sensitive TRPA1-expressing neurons mediate sensation of cold pain with the help of cold-resistant Na_V1.8 channel. The role of cold-insensitive TRPA1-expressing neurons in mediating cold pain remains unclear.

CHAPTER 6

FUTURE WORK

Now that we know the constellation of several ion channels and receptor in TRPM8- and TRPA1-expressing neurons, the question is do these constellations change under pathological conditions such as cold allodynia and hypersensitivity? Cold allodynia is a common side effect of platinum-based chemotheraphy drugs due to which patients undergoing treatment experience excruciating pain to non-painful or innocuous cold stimuli (Descoeur et al., 2011; Sittl et al., 2012). Although changes in expression and function of ion channels such as, TRPA1, TRPM8, K_V, and Na_V channels have been implicated, how these ion channels synergistically contribute to chemotherapy-induced neuropathy is not well understood (Descoeur et al., 2011; Nassini et al., 2011; Deuis et al., 2013; Boyette-davis et al., 2015). Hence, we plan to use constellation pharmacology and monitor functional expression of these ion channels in somatosensory neurons during chemotherapy treatment.

The constellation pharmacology platform has been useful for identifying cellular and molecular targets of natural products (Teichert et al., 2015). In fact, the inspiration for the constellation pharmacology platform came from marine cone snails that capture their prey by using a cocktail of peptides (cabals) acting on multiple ion channels and receptors simultaneously (Olivera et al., 2015). I am presently using constellation pharmacology for activity-guided fractionation of venom fractions of the predatory sea snail *Turridrupa elongata*. One of the venom fractions selectively activates (indirect effects by amplifying K+) a subset of TRPV1 expressing neurons. Hence, future experiments will focus on identifying the venom component responsible for these effects and its molecular target in TRPV1 expressing neurons.

6.1 References

Boyette-davis JA, Walters ET, Dougherty PM, Blvd H (2015) Mechanisms involved in the development of chemothreapy-induced neuropathy. Pain Manag 5:285–296.

Descoeur J, Pereira V, Pizzoccaro A, Francois A, Ling B, Maffre V, Couette B, Busserolles J, Courteix C, Noel J, Lazdunski M, Eschalier A, Authier N, Bourinet E (2011) Oxaliplatin-induced cold hypersensitivity is due to remodelling of ion channel expression in nociceptors. EMBO Mol Med 3:266–278 Available at: http://www.pubmedcentral.nih.gov/articlerender.fcgi?artid=3377073&tool=pmcentrez&rendertype=abstract [Accessed October 14, 2015].

Deuis JR, Zimmermann K, Romanovsky A a, Possani LD, Cabot PJ, Lewis RJ, Vetter I (2013) An animal model of oxaliplatin-induced cold allodynia reveals a crucial role for Nav1.6 in peripheral pain pathways. Pain 154:1749–1757 Available at: http://www.ncbi.nlm.nih.gov/pubmed/23711479 [Accessed November 13, 2013].

Nassini R, Gees M, Harrison S, De Siena G, Materazzi S, Moretto N, Failli P, Preti D, Marchetti N, Cavazzini A, Mancini F, Pedretti P, Nilius B, Patacchini R, Geppetti P (2011) Oxaliplatin elicits mechanical and cold allodynia in rodents via TRPA1 receptor stimulation. Pain 152:1621–1631.

Olivera BM, Safavi-Hemami H, Horvarth MP, Teichert RW (2015) Marine Biomedicine: From Beach to Bedside (Baker BJ, ed). CRC Press.

Sittl R, Lampert A, Huth T, Schuy ET, Link AS, Fleckenstein J, Alzheimer C, Grafe P, Carr RW (2012) Anticancer drug oxaliplatin induces acute cooling-aggravated neuropathy via sodium channel subtype $Na_V1.6$-resurgent and persistent current. PNAS 109:6704-6709.

Teichert RW, Schmidt EW, Olivera BM (2015) Constellation pharmacology : a new paradigm for drug discovery. Annu Rev Pharmacol Toxicol 55:573-589.